UNIVERSITY OF VERONA

DEPARTMENT OF MEDICINE

Graduate School Of Life And Health Sciences

Doctoral Program in Clinical and Experimental Biomedical Sciences

XXX Cycle, November 2014-October 2017

Heparanase regulates M1 macrophage polarization and the crosstalk between macrophages and tubular epithelial cells after kidney ischemia/reperfusion injury

S.S.D. MED/14

Coordinator: Prof. Giovanni Targher

Firma

Tutor: Prof. Gianluigi Zaza

Firma

PhD student: Dott.ssa Gloria Bellin

Firma

SOMMARIO

L'ischemia/riperfusione (I/R) è una condizione clinica causata da una riduzione di perfusione ad un tessuto seguito dal ripristino del flusso sanguigno, che si verifica in corso di infarto del miocardio, complicanze vascolari, trapianto d'organo e danno renale acuto.

Durante l'ischemia la riduzione di ossigeno e nutrienti causa l'alterazione del metabolismo e dell'omeostasi cellulare con attivazione del metabolismo anaerobio che porta ad una riduzione del pH, dell'ATP cellulare che inattiva le ATPasi, ad un sovraccarico di calcio e alla disfunzione mitocondriale che influisce ulteriormente sulla produzione di ATP. Inoltre l'ischemia attiva le principali pathway di morte cellulare: apoptosi, necrosi e autofagia.

Sebbene la riperfusione sia necessaria per ristabilire l'apporto di ossigeno e nutrienti al tessuto, essa esacerba il danno provocando il rilascio di specie reattive dell'ossigeno (ROS), il sovraccarico di calcio, la disfunzione endoteliale e la risposta infiammatoria, promuovendo così lo sviluppo di danni anche in altri organi.

Diversi studi hanno dimostrato che i macrofagi, grazie alla loro capacità di assumere un fenotipo pro-infiammatorio (M1) o pro-rigenerativo (M2) in risposta a differenti stimoli, svolgono un ruolo importante nel danno cellulare innescato dall'I/R infiltrandosi nel parenchima e promuovendo il danno tissutale.

Tuttavia i meccanismi biologici alla base di questa condizione non sono ancora del tutto chiari.

In questo processo l'eparanasi (HPSE), una endoglicosidasi che taglia le catene di eparan solfato regolando la biodisponibilità di fattori di crescita, lipoproteine, chemochine e citochine, sembra poter avere un ruolo importante.

Per comprendere il coinvolgimento di questo enzima nel processo infiammatorio indotto dal danno da I/R abbiamo valutato la capacità dell'HPSE e del suo specifico inibitore, SST0001, di modulare la polarizzazione dei macrofagi e il crosstalk tra macrofagi e cellule epiteliali del tubulo prossimale renale (HK-2) *in vitro* in un modello di ipossia /riossigenazione (H/R).

Inoltre, abbiamo valutato l'infiammazione renale, la polarizzazione dei macrofagi, e le modificazioni istologiche in un modello *in vivo* di topi sottoposti a I/R monolaterale e trattati con SST0001, sacrificati 2 o 7 giorni dopo l'I/R.

I risultati degli esperimenti *in vitro* hanno mostrato che l'HPSE sostiene la polarizzazione dei macrofagi verso il fenotipo M1 e la produzione di citochine proinfiammatorie da parte di questi. L'enzima promuove inoltre l'apoptosi, la sintesi e la produzione di damage associated molecular patterns (DAMP), la sintesi di citochine proinfiammatorie nelle cellule tubulari renali dopo H/R e l'iperespressione dei Toll-like receptors (TLRs) sia nelle cellule HK-2 che nei macrofagi. L'HPSE sembra promuovere anche la transizione epitelio-mesenchimale delle cellule tubulari renali mediata dai macrofagi M1. L'inibizione dell'HPSE *in vitro* blocca tutti gli questi effetti.

In vivo, l'inibizione dell'HPSE ha dimostrato di ridurre l'infiammazione e la polarizzazione dei macrofagi verso il fenotipo M1 dopo il danno da I/R, ristabilendo, almeno parzialmente, la funzione e la normale istologia renale e riducendo l'apoptosi.

Questi risultati mostrano per la prima volta che l'HPSE è in grado di mediare la polarizzazione dei macrofagi così come il danno renale dopo l'I/R.

In conclusione il nostro studio dimostra che l'HPSE è un elemento chiave coinvolto nei complessi processi biologici attivati dal danno da I/R, regolando las attivazione/polarizzazione dei macrofagi e il crosstalk tra queste cellule infiammatorie e l'epitelio tubulare renale.

Inoltre, i risultati di questo studio suggeriscono che l'inibizione dell'HPSE, mitigando i danni morfologici e funzionali dovuti al danno da I/R, potrebbe rappresentare un nuovo strumento farmacologico nella medicina dei trapianti. Ulteriori studi e trial clinici sono necessari per confermare i nostri risultati.

ABSTRACT

Ischemia/reperfusion (I/R) is a clinical condition characterized by a decrease of tissue perfusion and the subsequent restoration of blood flow. This event occurs in myocardial infarction, major vascular surgery complication, organ transplantation and acute kidney injury (AKI).

During ischemia the reduction of oxygen and nutrients cause alteration of cell metabolism/energy and homeostasis with the activation of anaerobic metabolism leading to decreased pH, the depletion of cellular ATP which inactivates ATPases, calcium overload, and mitochondrial dysfunction that further impairs ATP production. Moreover, ischemia activates cell death programs: apoptosis, necrosis and autophagy-associated cell death.

Even if reperfusion is necessary to re-establish oxygen and nutrients supply to the tissue, it exacerbates the injury with the release of reactive oxygen species (ROS), calcium overload, endothelial dysfunction and a pronounced inflammatory response promoting damages also in other organs.

In this process Heparanase (HPSE), an endoglycosidase that cleaves heparan sulfate chains modulating extracellular matrix, seemed to have a pivotal role.

Additionally, many studies have shown that macrophages, thanks to their ability to switch between M1 proinflammatory and M2 pro-regenerative phenotypes in response to different stimuli, are involved in the disrupted cellular network triggered by I/R, by infiltrating into renal parenchyma and causing tissue damage. However, although well described, the biological mechanisms underlining this process are still only partially understood.

To better assess this object, we measured the capability of HPSE and its inhibitor, SST0001, to control macrophage polarization and the crosstalk between macrophages and HK-2 renal tubular cells during *in vitro* hypoxia/reoxygenation (H/R). Besides, we gauged *in vivo* renal inflammation, macrophage polarization, and histologic changes in mice subjected to monolateral I/R and treated with SST0001 for 2 or 7 days.

The in *vitro* experiments displayed that HPSE sustained M1 macrophage polarization, enhancing their production of proinflammatory cytokines.

Furthermore, it modulated apoptosis, the synthesis/production of damage associated molecular patterns (DAMPs) and the synthesis of proinflammatory cytokines in post-H/R tubular cells, and the upregulation of TLRs on both epithelial cells and macrophages. HPSE also regulated M1 polarization induced by H/R-injured tubular cells and the partial epithelial–to-mesenchymal transition (EMT) of these epithelial cells by M1 macrophages. All these effects were disallowed by blocking HPSE. Additionally, the inhibition of HPSE *in vivo* reduced inflammation and M1 macrophage polarization in mice undergoing I/R injury, partially re-established renal function and normal histology, and decreased apoptosis. These results show for the first time that HPSE is able to mediate macrophage polarization as well as renal damage and repair after I/R.

In conclusion, our study demonstrated that HPSE is a pivotal element involved in the complex renal biological machinery activated by I/R injury by regulating macrophages polarization/activation and the crosstalk between these immune-inflammatory cells and the renal tubular epithelium. Furthermore, it underlined that the inhibition of this enzyme, mitigating functional and morphological damages following I/R injury, could represent a new pharmacological tool in organ transplant medicine. Additional studies and trials are necessary to confirm our results in clinical setting.

TABLE OF CONTENTS

List of abbreviations

α-SMA alpha smooth muscle actin

AIF Apoptosis-inducing factor

AKI Acute kidney injury

ATP Adenosin triphosphate

BCA Bicinchoninic acid

bFGF Basic fibroblast growth factor

BSA Bovine serum albumin

BUN Blood urea nitrogen

CAN Chronic allograft nephropathy

CASP Caspase

CKD Chronic kidney disease

DAMPs Damage associated pattern molecules

DC Dendritic cells

DGF Delayed graft function

DISC Death inducing signaling complex

DTT Dithiothreitol

ECM Extracellular matrix

ELISA Enzyme-linked immunosorbent assay

EMT Epithelial-mesenchymal transition

ER Endoplasmatic reticulum

FBS Fetal bovine serum

FGF-2 Fibroblast growth factor-2

FGFR1 Fibroblast growth factor receptor-1

FN Fibronectin

GBM Glomerular basament membrane

H_2O_2 Hydrogen peroxide

HIF Hypoxia inducible factor

HK-2 Human kidney tubular epithelial cells

$HOO^{\bullet}$ Hydroperoxyl radical

HPSE Heparanase

HS Heparan sulfate

HSPG Heparan sulfate proteoglycan

H/R Hypoxia/reperfusion

IF Immunofluorescence

IFN-γ Interferon gammaγ

IL Interleukin

iNOS Inducible nitric oxide synthase

I/R Ischemia/reperfusion

IRI Ischemia/reperfusion injury

LMWH Low molecular weight heparin

LPS Lipopolysaccharide

MCP-1 Monocite chemoattractant protein

MMP Matrix metalloprotease

MPTP Mitochondrial permeability transition pore

NAD Nicotinamide adenine dinucleotide

NADPH Nicotinamide adenine dinucleotide phosphate

NF-kB Nuclear factor kappa

NK Natural killer

NO Nitric oxide

Nox NAPH oxidase

O_2^- Superoxide anion radical

$^{\bullet}$OH Oxydril radical

$ONOO^-$ Peroxinitrite anion

ONOOH Peroxynitrous acid

PAS Periodic Shiff's acid

PBS Phosphate buffered saline

PMA Phorbol myristate acetate

PRR Pattern recognition receptor

ROS Reactive oxygen species

RT Room temperature

RT-PCR Reverse transcriptase-polymerase chain reaction

SDC Sindecan

TBS Tris buffered saline

TBST Tris buffered saline Tween-20

TGF-β Transforming growth factor beta

TLR Toll-like receptor

TNF-α Tumor necrosis factor alpha

VEGF Vascular endothelial growth factor

VIM Vimentin

1. INTRODUCTION

1.1. Ischemia/Reperfusion Injury

Ischemia/reperfusion (I/R) is a clinical condition characterized by a decrease of tissue perfusion and the subsequent restoration of blood flow. This event occurs in myocardial infarction, major vascular surgery complication, organ transplantation and acute kidney injury (AKI).

During ischemia the reduction of oxygen and nutrients cause alteration of cell metabolism/energy and homeostasis [1] with the activation of anaerobic metabolism leading to decreased pH, the depletion of cellular ATP which inactivates ATPases (e.g., Na+/K+ ATPase), calcium overload, and mitochondrial dysfunction that further impairs ATP production. Moreover ischemia activates cell death programs: apoptosis, necrosis and autophagy-associated cell death [2].

Even if reperfusion is necessary to re-establish oxygen and nutrients supply to the tissue, it exacerbates the injury with the release of reactive oxygen species (ROS), calcium overload, endothelial dysfunction and a pronounced inflammatory response [3] promoting damages also in distant organs [4] (Fig. 1).

1.1.1. Mechanisms involved in I/R injury

The mechanisms underlying I/R injury (I/R injury) are complex, multifactorial and highly integrated. They include the perturbation of calcium (Ca^{2+}) homeostasis, production of ROS, the activation of apoptotic and autophagic pathways, and inflammation (Fig. 1).

1.1.1.1. Calcium homeostasis

During ischemia, the production of ATP by anaerobic glycolysis causes accumulating lactate, protons and NAD^+ and consequent fall in intracellular pH. In order to re-establish normal pH, the cell extrudes H^+ ions in exchange for Na^+ via the plasmalemmal Na^+/H^+ exchanger [5-7]. The Na^+ ions are, in turn,

exchanged for Ca^{2+} by the plasmalemmal Na^{+}/Ca^{2+} exchanger. Increased intracellular Ca^{2+} activates several pathways contributing to cell death and organ dysfunction.

1.1.1.2. Oxidative stress

The reintroduction of molecular oxygen to the tissues exacerbates the ROS production that play an important role in tissue injury. The primary ROS produced in I/R, by the univalent reduction of a molecule of oxygen, is the superoxide anion radical (O_2^-) made by cytosolic and membrane enzymes (xanthine oxidase, NADPH oxidase, cytochrome P450 oxidases, and uncoupled nitric oxide synthase), as well as via the electron transport chain in mitochondria. It is rapidly converted into hydrogen peroxide (H_2O_2) spontaneously, or by superoxide dismutase [8]. However, especially in low pH condition, O_2^- can be converted into hydroperoxyl radical ($HOO^{\bullet}$), a potent oxidant. O_2^- can react with nitric oxide (NO), forming peroxinitrite anion ($ONOO^-$) which can be protonated to the highly cytotoxic peroxynitrous acid (ONOOH) or transformed in oxydril radical ($^{\bullet}OH$), that is an important modulator of cell signalling [4].

ROS induce tissue dysfunction by directly damaging cells via numerous mechanisms including peroxidation of cell membrane and organelle lipids, oxidation of DNA, activation of matrix metalloproteinases and calpains, producing osmotic cell lysis, and opening of the mitochondrial permeability transition pore [9]. ROS may also induce cell dysfunction and death by indirect mechanisms through the interaction with NO, fatty acids or free iron to form peroxynitrite, peroxyl radicals, and hydroxyl radicals, respectively, each of which are capable of producing even more cellular damage than superoxide or hydrogen peroxide. ROS enhance the inflammatory response during reperfusion via formation of oxidant-dependent proinflammatory mediators and upregulation of cytokines/chemokines and adhesion molecules expression [9].

1.1.1.3. Apoptosis and autophagy

Ischemia and reperfusion activate several stimuli that lead to cell death through apoptosis, necrosis and autophagy.

Apoptosis is characterized by morphological features such as membrane blebbing, chromatin condensation, nuclear condensation and cell shrinkage without the activation of an inflammatory process. This form of cell death requires caspases (CASP) activation, as these enzymes can activate the endonucleases responsible for DNA degradation [10]. During I/R injury both intrinsic and extrinsic apoptotic pathways are activated.

Ca^{2+} overload and oxidative stress cause the opening of mitochondrial permeability transition pore (MPTP) with consequent mitochondria depolarization and the release of cytochrome c and apoptosis-inducing factor (AIF) that activate, respectively, caspase-dependent and caspase-independent cell death programs [11, 12].

Beyond direct effects on mitochondria, calcium may activate phospholipases and calpains, which in turn cause the processing and release of the mitochondrial protein AIF which translocates to the nucleus to mediate DNA fragmentation [13].

For the extrinsic pathway, the upregulation of Fas and Tumor necrosis factor-α (TNF-α) receptor and their ligands during I/R leads to the formation of death inducing signaling complex (DISC) activating CASP-8 which, in turn, cleaves and activates CASP-3.

The extrinsic and intrinsic pathways lead to activation of CASP-3 that causes cell shrinkage and nuclear fragmentation within the apoptotic cell.

Necrosis is a faster process with early membrane failure, cell swelling and the release of cellular debris, leading to tissue infiltration of inflammatory-cells with consequent cytokines release [14].

Autophagy is the tightly regulated intracellular catabolic process that serves as the cellular quality control mechanism for the removal of damaged and dysfunctional organelles and protein aggregates, that activate it [15]. Autophagy is both a survival and death mechanism: in stressful condition as like as I/R, autophagy helps cell survival by removing damaged organelles and intracellular pathogens, and generating amino acids and fatty acids. However, uncontrolled autophagy leads to cell death [4].

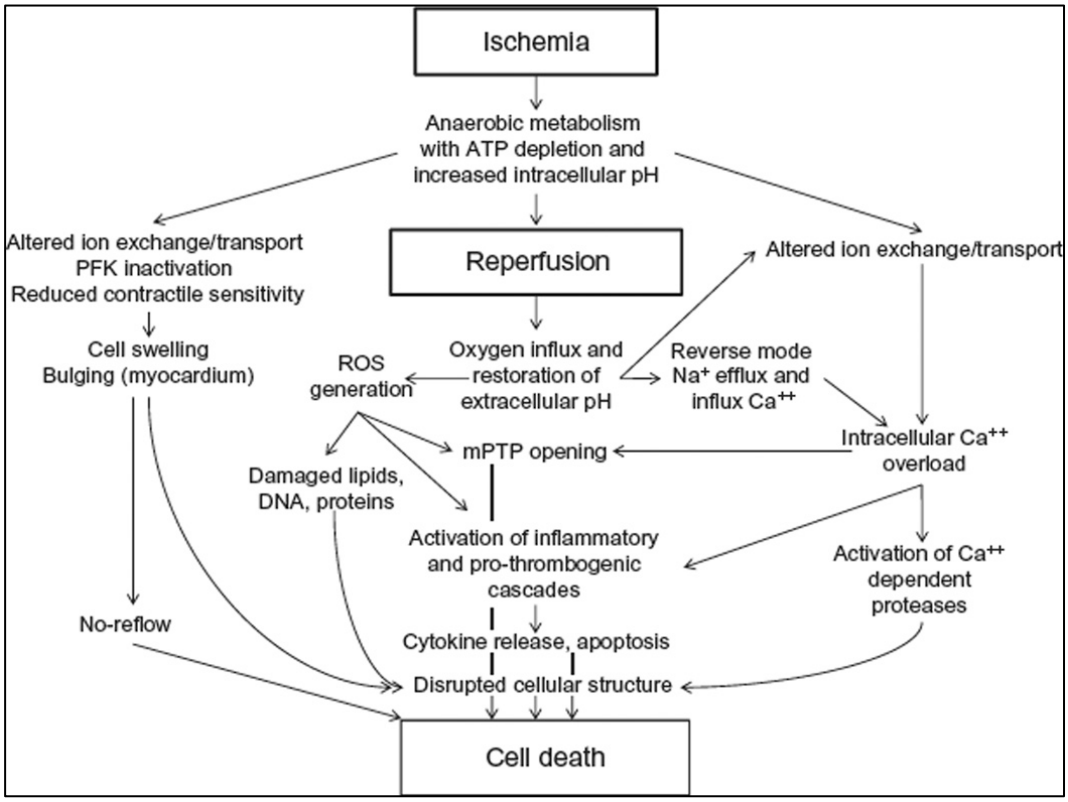

Fig. 1: Major pathologic events contributing to I/R. Cells under ischemic condition undergo anaerobic metabolism which alters intracellular pH and Ca^{2+} homeostasis. The subsequent reperfusion leads to the production of a wide amount of ROS which promote DNA, proteins and lipids damages; as a consequence, inflammatory response is activated. These series of events promote cell death. From [4].

1.1.1.4. Inflammation

Inflammation is one of the most important factors triggered by I/R.

Following I/R inflammation occurs in absence of pathogens and is activated by danger signals from injured cells. It is characterized by the production of proinflammatory cytokines and chemokines, and is orchestrated by several cell types: neutrophils, dendritic cells, natural killer cells, platelets and macrophages.

1.1.1.4.1. Neutrophils

Neutrophils are the largest circulating fraction of leukocytes and the first to arrive at the site of injury [16].

Neutrophils are recruited by signals provided by chemokines that are produced by tissue resident macrophages and endothelial cells [17]. Once neutrophils

transmigrate through the endothelium, they release the content of their granules containing proteases and release ROS through the 'respiratory burst'. Moreover additional leukocytes are recruited through the production of cytokines and chemokines by neutrophils [18].

1.1.1.4.2. Dendritic cells

Dendritic cells (DCs) originate from circulating mononuclear phagocytes that, once infiltrated into injured tissue, can differentiate into DCs or macrophages. They orchestrate the adaptive response representing a link between innate and adaptive immunity. In the context of organ transplantation, DCs derived from donor tissue have the capacity to activate pattern recognition receptors (PRRs) following I/R injury, however, they are also capable of modulating peripheral T-cell tolerance playing a protective role [19, 20].

1.1.1.4.3. Natural killer cells

Natural killer (NK) cells are lymphocytes capable of distinguish between "self" and "non-self" by the activation or the inhibition of cell surface receptors through the major histocompatibility complex 1 (MHC-I) [21]. In a renal model of I/R injury, NK cells seem to be recruited by the production of the chemokine CCR5 released by tubular epithelial cells after Toll-like receptor (TLR)-2 activation; moreover they contribute to the injury stimulating the production of additional chemokines by tubular epithelial cells [22, 23]. It has been reported also that NK cells directly stress epithelial cells by inducing their apoptosis [18].

1.1.1.4.4. Platelets

Several studies underlined the role of platelets on inflammatory response in I/R injury, in addition to their role on thrombogenesis. Upon tissue damage, activated platelets aggregate and adhere to the endothelium, to leukocytes and lymphocytes through P-selectin and integrin-mediated mechanisms, and it seems to mediate leucocytes transmigration [24, 25]. Furthermore, platelets release a number of pro-inflammatory factors such as Interleukin (IL)-1β, RANTES, H_2O_2 and proapoptotic molecules that directly enhance inflammation [4].

1.1.1.4.5. Macrophages

Macrophages are a critical component of the phagocytic system involved in the inflammatory response. They can be resident in the tissues or can originate from circulating monocytes that, once infiltrate in the site of injury, differentiate into macrophages [26]. They exhibit a high degree of plasticity and in response to different local microenvironments, resting macrophages can polarized into different phenotypes, proinflammatory (M1) or anti-inflammatory (M2) with different role [27].

M1 macrophages are induced by lipopolysaccharide (LPS) or interferon-γ (IFN-γ), they enhance the early inflammatory response producing pro-inflammatory mediators including IL-1β, IL-6, TNF-α, and MCP-1, and are characterized by the expression of inducible nitric oxide synthase (iNOS).

M2 macrophages are induced by IL-4 and IL-10 [28] and play a role in the second phase of inflammation. They have an anti-inflammatory function and are involved in wound healing, tissue regeneration, but also fibrosis [29]. M2 macrophages are characterized by the expression of mannose receptor (MR) (in human) or Arginin 1 (Arg1) (in mice), that represent the M2 markers [30].

After I/R injury, macrophages exposed to inflammatory environment assume the M1 phenotype and produce, together with the other inflammatory cells, pro-inflammatory cytokines. In a model of renal I/R the depletion of macrophages prior to I/R ameliorated the injury. In contrast, if macrophages were depleted even days after I/R injury tubular proliferation and repair resulted impaired, because of the depletion of M2 macrophages [31]. This suggests that M1 macrophages play an important pathological role in the early stage of injury, while in the late stage M2 macrophages promote tissue repair.

1.1.2. I/R injury in kidney

In renal transplantation, the development of the I/R injury is often followed by important pathophysiological alterations that can lead to acute impairment and trigger pro-fibrotic pathways. The latter may be responsible of an early onset and development of the chronic allograft nephropathy (CAN) [32].

Particularly, I/R injury is implicated in a severe clinical complication of the first post-transplant stage namely delayed graft function (DGF) [32], characterized by a strong association with both acute rejection and decreased graft survival [33-36]. In the long term, patients with DGF are approximately 1.5 times more susceptible to graft loss at 5 years, and present an overall 10% lower graft survival rate compared to patients with early graft function [33, 37, 38]. Because of the negative impact of DGF on both short and long-term graft outcome, great efforts have been made to identify factors associated with DGF, and to identify valuable easy clinical/biological algorithms to predict this condition [39-41], but, at the moment, no suitable biomarkers have successfully entered in routine clinical practice.

As shown by the transcriptomic profile of pre-transplant biopsy, several donor (e.g., age, diabetes, hypertension) and graft characteristics together with length of cold ischemia time are involved in the biological machinery leading to DGF, but also recipients' conditions may have a pivotal role [36].

Our group has recently demonstrated that an upregulation of some cellular elements (karyopherins) in immune cells of dialyzed chronic kidney disease (CKD) patients could predispose them to develop DGF in the post-transplant period [42, 43].

Additionally, the ischemic phase induces apoptosis and/or necrosis of tubular epithelial cells with a consequent release of danger-associated molecular patterns (DAMPs), such as hyaluronic acid, fibronectin (FN), heat shock proteins (HSP), and DNA which activate TLR-2 and -4, and the PRR [44]. All of them may activate cell death signalling pathways and intra-cellular proinflammatory networks [45].

Mostly, when engaged, TLRs elicit the production of several proinflammatory cytokines, such as TNF-α, IL-1β, IL-6, CCL2, MIP-2, and chemokines further accompanied by neutrophil and macrophage infiltration [26, 27, 46, 47]. Additionally, I/R may activate the intra-parenchymal complement system that can exacerbate tissue damage [46].

Moreover, the abovementioned biological machinery may determine a pro-fibrogenic tissue response. This is characterize by four major phases: 1) primary injury of the organ; 2) persistent parenchymal cells injury that stimulate the activation of effector cells into fibrogenic myofibroblast; 3) extra cellular matrix (ECM) is elaborated from myofibroblasts which produce α-smooth muscle actin (α-SMA) and secrete a high amount of collagen, FN and laminin; 4) the large deposition of ECM together with its insufficient degradation are responsible for the progression to fibrosis up to organ deformation and failure [48, 49]. Myofibroblasts sources include resident fibroblast, fibrocytes, pericytes and also epithelial cells undergoing epithelial to mesenchymal transition (EMT) [50]. During EMT epithelial cells are characterized by the gradual loss of epithelial proteins E-cadherin, zonula occludens-1 (ZO-1), cytokeratin and the acquisition of mesenchymal markers as like as α-SMA, FN, vimentin (VIM) and fibroblast specific protein-1 (FSP-1) (Fig. 2) [51].

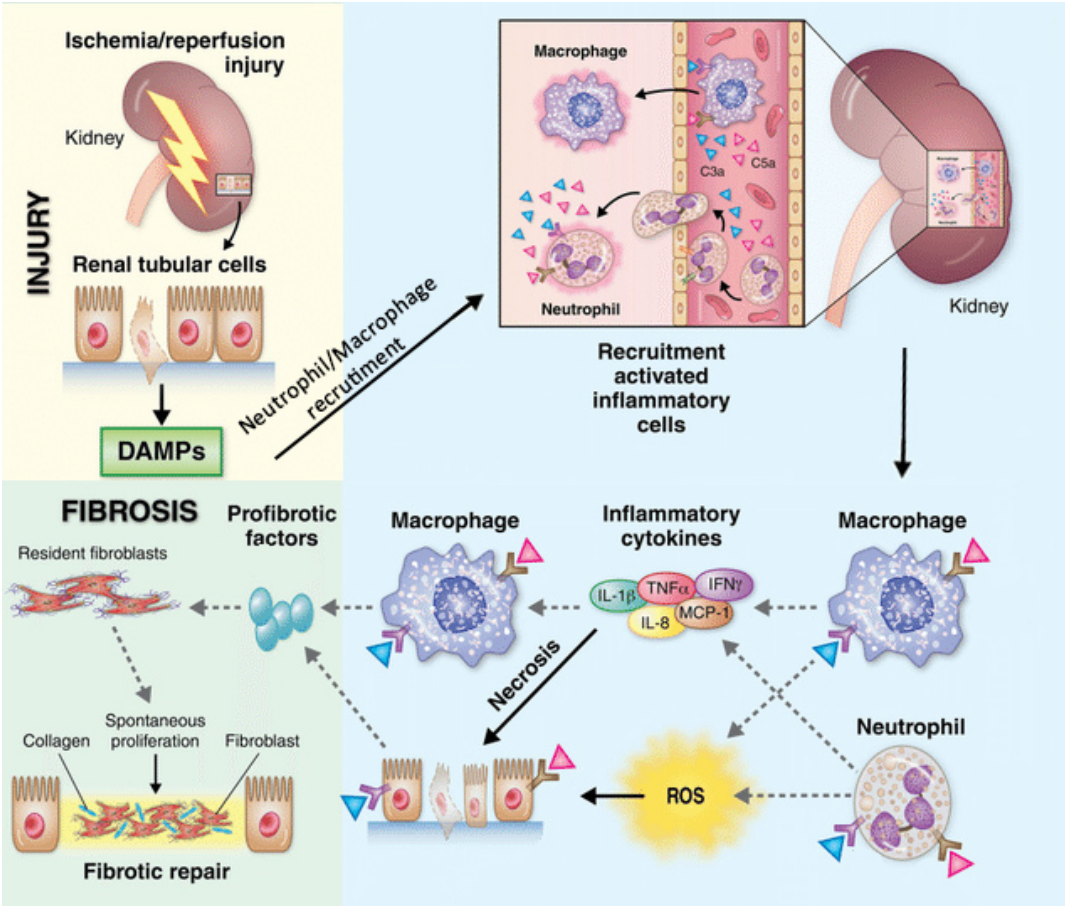

Fig. 2: Renal ischemia-reperfusion injury. Ischemia-reperfusion injury causes the generation and the release of DAMPs from renal injured cells, which promote inflammatory cells recruitment and release of proinflammatory cytokines and chemokines and enhances the production of ROS, intensifying the immune response and further amplifying the level of tubular necrosis and apoptosis. Activated endothelium, monocytes and injured tubular epithelium have all been shown to secrete pro-fibrogenic factors which in turn activate local fibroblasts and lead tubular cells to EMT, inducing collagen deposition and tissue repair. Modified from [46]

1.1.3. Inflammation in renal I/R injury

Both innate and adaptive immune responses are important contributors to the pathology of renal I/R injury. The innate component is responsible for the early response to injury and comprises neutrophils, monocytes/macrophages, DCs, NK cells. Neutrophils attach to the activated endothelium and accumulate in the kidney particularly in the peritubular capillary network of the outer medulla, as early as 30 minutes after reperfusion. They produce proteases, myeloperoxidase, ROS, and cytokines, which leads to increased vascular permeability and reduced tubular epithelial and endothelial cell integrity [52], aggravating renal injury [53].
Endothelial cells increase the expression of chemokine fractalkine (CX3CL1) that interacts with the receptor CX3CR1 on macrophages membrane, favouring their migration into interstitial tissues [54].
Macrophages enhance the inflammatory cascade by producing proinflammatory cytokines and have an important role in I/R injury.
Activation of TLRs by damaged renal tubular epithelial cells and IFN-γ secreted by NK cells promotes full activation of M1 macrophages [55], that predominate during the early injury phase, when tubular apoptosis is prominent.
Conversely, during the tubular repair phase, when tubular cells are proliferating and repopulating the denuded basement membrane, renal macrophages express markers of M2 phenotype. It has been demonstrated that proximal tubular epithelial cells promote this process through the production of GM-CSF [27].
Interestingly in a study with I/R injury for 8 weeks, Ko and his colleagues showed that macrophage depletion attenuates inflammation and tubulointerstitial fibrosis with a decrease in the expression of inflammatory and profibrotic cytokines [56], suggesting that macrophages are involved in both the early inflammation and later fibrogenesis.
If the inflammatory process becomes deregulated because of the persistence of M1 macrophages, AKI can get on CKD and can promote the development of fibrosis (Fig. 3).

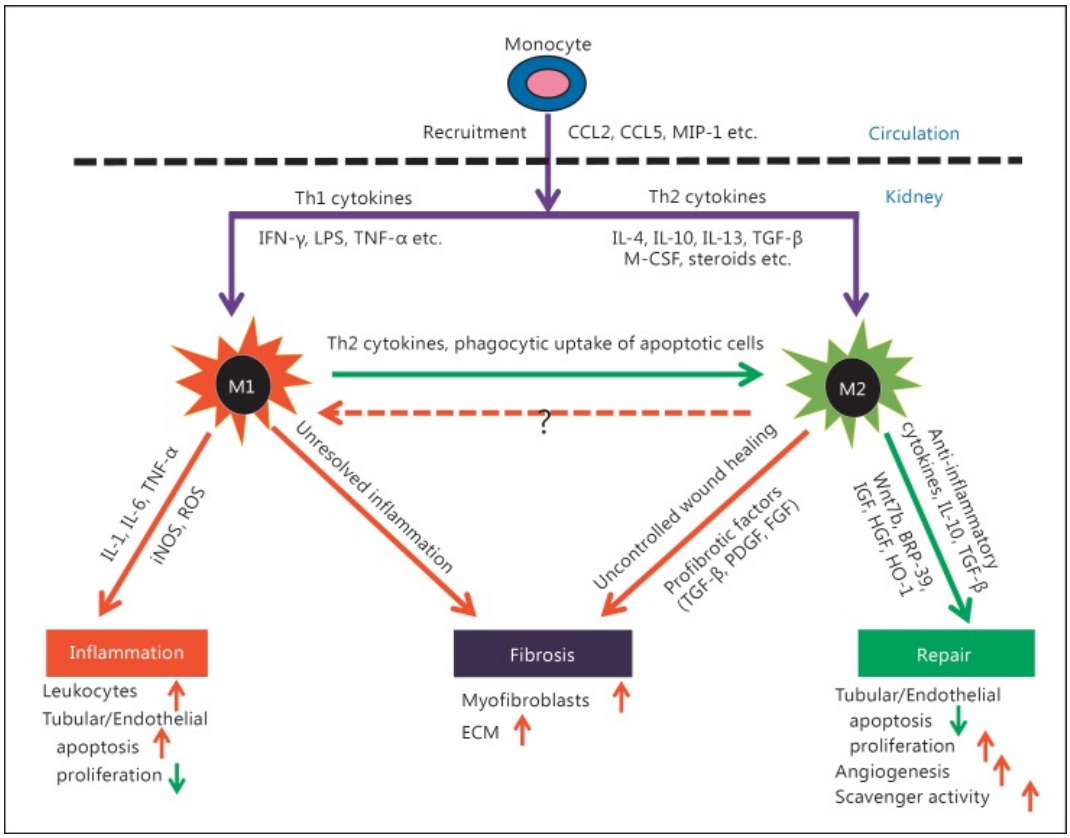

Fig. 3: Macrophages polarization during injury and repair. During renal inflammation, circulating monocytes are recruited into the kidney because of the release of cytokines and chemokines by neutrophils and kidney resident cells. They differentiate into macrophages and polarize to distinct phenotypes under the influence of local microenvironments. Th1 proinflammatory cytokines (such as IFN-γ and TNF-α) induce M1 macrophages, while Th2 anti-inflammatory cytokines (such as IL-4, IL-13, and IL-10) promote M2 polarization. Moreover, the uptake of apoptotic cells and the production of Th2 cytokines can cause the switch from M1 to M2 phenotype. M1 macrophages produce an abundance of proinflammatory cytokines (IL-1, IL-6, and TNF-α), iNOS, and ROS, promoting renal injury, while M2 macrophages synthesize anti-inflammatory cytokines (IL-10 and TGF-β) and trophic factors. However, unresolved inflammation and uncontrolled wound healing processes can trigger the process of renal fibrosis by enhancing activation and differentiation of macrophages. From [57].

1.2. Heparanase

Heparanase (HPSE) is the only known mammalian endo-β-D-glucuronidase capable of cleaving (HS) side chains of Heparan Sulfate Proteoglycans (HSPGs) [58]. It belongs to the clan A glycosyl hydrolase family [59]. This enzyme participates in the remodelling of ECM and regulates the bioavailability of several molecules such as growth factors, lipoproteins, chemokines and cytokines that are released following HS degradation.

HS is a polysaccharide presents in the ECM and in cellular surface in the form of proteoglycan. It binds several molecular factors, regulating a lot of biological activities such as angiogenesis, fibrosis and tumour metastasis.

In detail HPSE cleaves HS chains catalyzing the hydrolysis of the β-glycosidic bond at specific intrachain sides yielding 5-7 kDa fragments [60, 61]. HPSE acts also on heparin, generating fragments of 5-20 kDa [62].

1.2.1 Heparanase expression, biogenesis and structure

HPSE primary structure is highly conserved in different species like mammals, chicken and zebrafish. Human HPSE is encoded by a single copy of HPSE gene, located on chromosome 4q22, which encodes the 1a and 1b spliced mRNA isoforms [63].

In normal cells and tissues the HPSE promoter is silenced by methylation and p53 antigen except for placenta, activated immune cells and keratinocytes where HPSE is constitutively active [64]. In other cell types and tissues the expression of HPSE can be induced by different mediators through the activation of NF-kB transcription factor [65].

HPSE is produced as a 543 amino acids pre-pro-enzyme. Upon translocation into the endoplasmatic reticulum, the N-terminal signal peptide (Met1-Ala35) is removed and the latent 65 kDa pro-HPSE is generated. The pro-enzyme is transferred to the Golgi apparatus, encapsulated in vesicles and secreted [60]. It interacts with different extracellular components among which HS and HSPGs such as syndecan-1 (SDC-1). Once formed, HPSE-syndecan complex is rapidly

internalized into lysosomes and endosomes, leading to its processing and activation mediated by cathepsin L at perinuclear localization [66, 67]. Then HPSE can be carried on the cellular surface or released into the ECM where it exerts its activity of cleaving HS (Fig. 4).

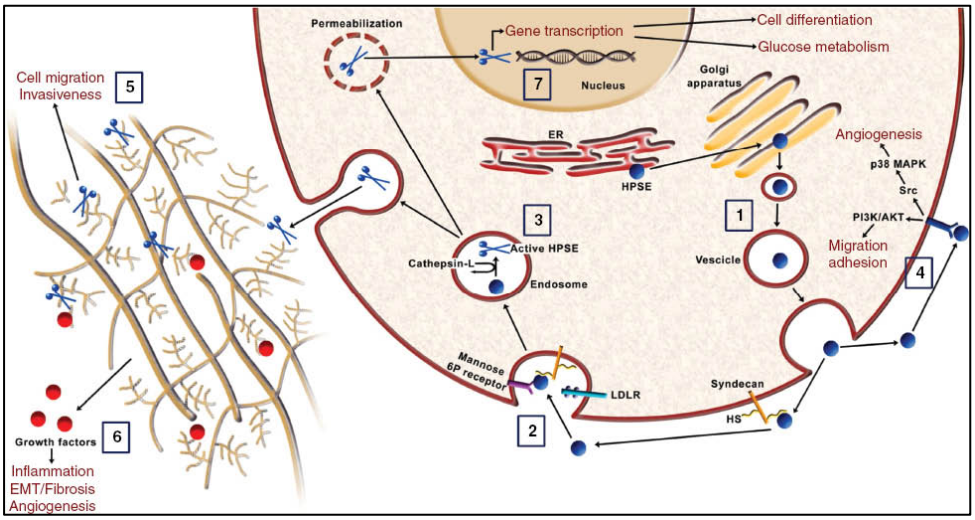

Fig. 4: HPSE processing, localization, enzymatic and non-enzymatic activities. HPSE is synthesized in the endoplasmic reticulum as a latent precursor. After moving to the Golgi apparatus, pro-HPSE is secreted outside the cell (1). HPSE is then uptaken [by syndecans, mannose-6-phosphate-receptor and low-density lipoprotein receptor (LDLR)-related protein] (2), and delivered to lysosome where it is proteolytically processed by cathepsin-L and converted to the active enzyme (3). The interaction of latent HPSE with HPSE-binding proteins activates various intracellular signaling pathways implicated in angiogenesis, cell adhesion and migration (4). Extracellular HSPGs degradation encourages cell migration, thus enhancing tumor cell invasiveness and metastasis (5). Angiogenesis, EMT and inflammatory response are indirectly regulated by HPSE via HS-linked growth factors that are released after HS cleavage (6). Nuclear HPSE translocation is implicated in cell differentiation, inflammation and glucose metabolism through gene transcription regulation mechanisms (7). From [49].

Activated HPSE is a noncovalent heterodimer composed of the N-terminal 8 kDa (Gln36-Glu109) chain and the C-terminal 50 kDa (Lys158-Ile543) chain [68]. The proposed 3D structure, confirmed by the crystallography analysis, is a $(\beta/\alpha)_8$-TIM barrel fold. The first three alternated β-strands/α-helices belong to the 8 kDa chain, the other five are provided by the 50 kDa chain [69, 70]. The 50 kDa chain folds

also into a carboxy-terminal β-sandwich domain, essential for protein secretion, enzymatic and non-enzymatic activity (Fig. 5) [71].

The proteolytic activation of HPSE displays a ≈ 10Å cleft containing the HS-binding site, more precisely a catalytic nucleophile and proton donor site consisting of Glu_{343} and Glu_{225} residues [59, 69]. Besides, Levy-Adam *et al.* identified two other residues, Lys_{158} and Lys_{159}, close to the active site, that are very important for heparanase-heparin/HS interaction and as a consequence for HPSE inhibition strategies [72].

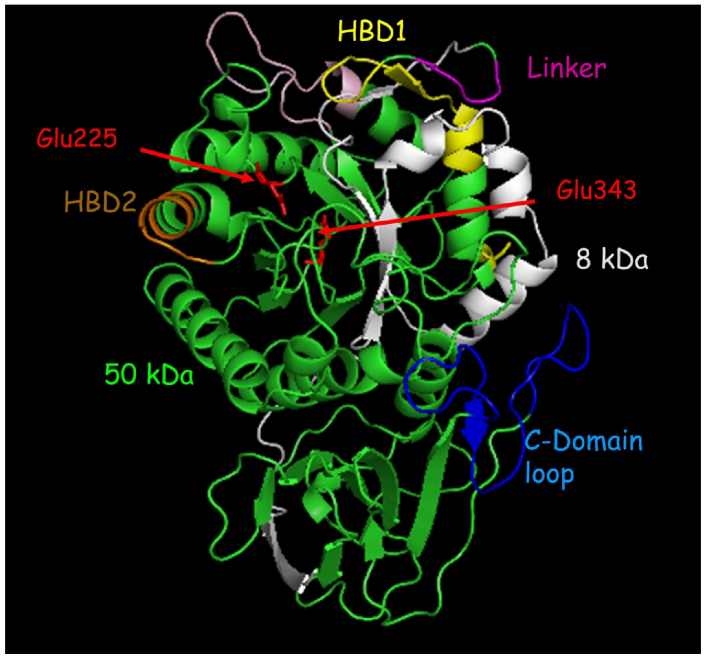

Fig. 5: Crystal structure of heparanase. Heparanase is composed of a TIM-barrel fold which contains the active site of the enzyme and a C-terminus domain required for secretion and signaling function of the protein. Heparanase has a catalytic mechanism which includes a putative proton donor at Glu_{225} and a nucleophile at Glu_{343} (red) as well as the heparin/heparan sulfate binding domains (HBD1 = Lys_{158}-Asp_{171}& HBD2 = Gln_{270}-Lys_{280}; yellow and brown, respectively) that are located in close proximity to the active site micro-pocket fold. The C-domain is comprised of 8 β-strands arranged in two sheets, as well as a flexible, unstructured loop that lies in-between (blue). Notably, the 8 kDa subunit (grey) enfolds the 50 kDa subunit (green), contributing β/α/β unit to the TIM-barrel fold and, moreover, one of the 8 β strands that comprise the C-domain. From [73].

1.2.2. Heparanase activity

HPSE catalyses the cleavage of HS chains present in pericellular space (perlcan) and cell surface (glypican). More precisely, HPSE recognizes a specific site on HS, a tetrasaccharide that forms a HPSE binding cleft. The enzyme binds to this cleft and cleaves the glycosidic bond between glucuronic acid (GlcA) and *N*-sulfated/6-*O*-sulfated glucosamine or *N*-acetylated/6-*O*-sulfated glucosamine [69, 74] (Fig. 6).

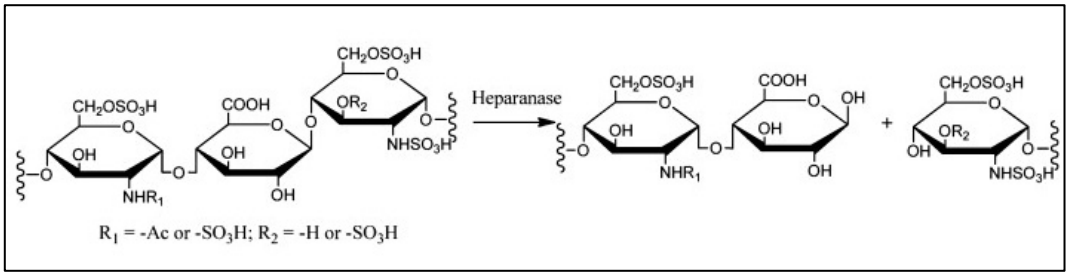

Fig. 6. The structure of HS and the reactions catalyzed by heparanase. Modified from [75].

By its enzymatic activity HPSE participates at the turnover of HSPGs on cell surface and matrix, promotes the remodelling of ECM and basal membrane, and the release of HS-linked growth factors, chemokines and cytokines into the local environment. In this way HPSE favours cells migration and proliferation, but also neovascularization and inflammation [60].

1.2.2.1. Strategies for heparanase inhibition

In the last two decades several classes of HPSE inhibitors have been developed ranging from monoclonal antibodies, nucleic acid, small-molecules to polysulfated saccharides-molecule inhibitors.

Antibodies against HPSE are an efficient strategy to inhibit its activity; recently two monoclonal antibodies were described: one against the KKDC peptide and the other against the full-length HPSE protein. They resulted able to neutralize extracellular HPSE and to decrease its intracellular content [76]. The combined application of the two antibodies seems to limit tumour growth, favouring the development of novel antibodies or combination with small-molecules inhibitors.

Small-molecules inhibitors are characterized by high variability in molecular weight; relevant functional group and physiochemical properties supporting the idea that HPSE could be inhibited by several mechanisms and several compounds with different structures [60].

Another approach, developed for basic research but not yet tested in clinical trial, is based on the inhibition of HPSE gene expression by antisense oligonucleotide, aptamers, siRNAs, shRNAs and miRNAs. This strategy results to prevent different cancer cell lines proliferation and invasiveness and to reduce tumour growth and angiogenesis in *in vivo* models [77-79].

In the last few years vaccination against HPSE was also investigated, not only as therapeutic but also as preventive strategy. Immunized serum showed to decrease invasiveness of melanoma cell line and profilactic vaccination significantly reduced tumour growth and metastasis in treated mice [80].

However, the only HPSE inhibitor compounds reaching the phase of clinical trial belong to the class of polysaccharides. The development of these compounds is based on the capacity of heparin to inhibit HPSE activity due to competition with HS for binding to the enzyme. Heparin contains some saccharide sequences recognized and cleaved by HPSE, and therefore it acts as a substrate for this enzyme. However, its peculiar anticoagulant activity hampered its pharmacological activity [60].

This has led to apply and evaluate heparin modifications, looking for new compounds. Improved inhibitory functions were attributed at the glycol-split heparins because of their higher conformational freedom conferred by the split portions, which favour the accommodation of polysaccharide chain within the HPSE binding site [81]. Currently, four HPSE-inhibitors are being trailed: PI-88, PG545, SST0001 and M402 (Fig. 7).

PG545 is a fully sulphated HS mimetic, able to inhibit HPSE enzymatic function on HS chain. It is in Phase I clinical trial against solid tumours [82, 83].

SST0001-ronepartat is a semisynthetic heparin-like polymer transformed into a 15-25 kDa glycol-split *N*-acetyl heparin. With reduced anticoagulant properties and a powerful anti-HPSE activity [81]. It is in Phase I study with dexamethasone in patients with advance multiple myeloma.

M402-necuparanid is another glycol-split HS mimetic with low molecular weight (5-8 kDa). It is currently under Phase II trial investigation in patients with pancreatic cancer [60].

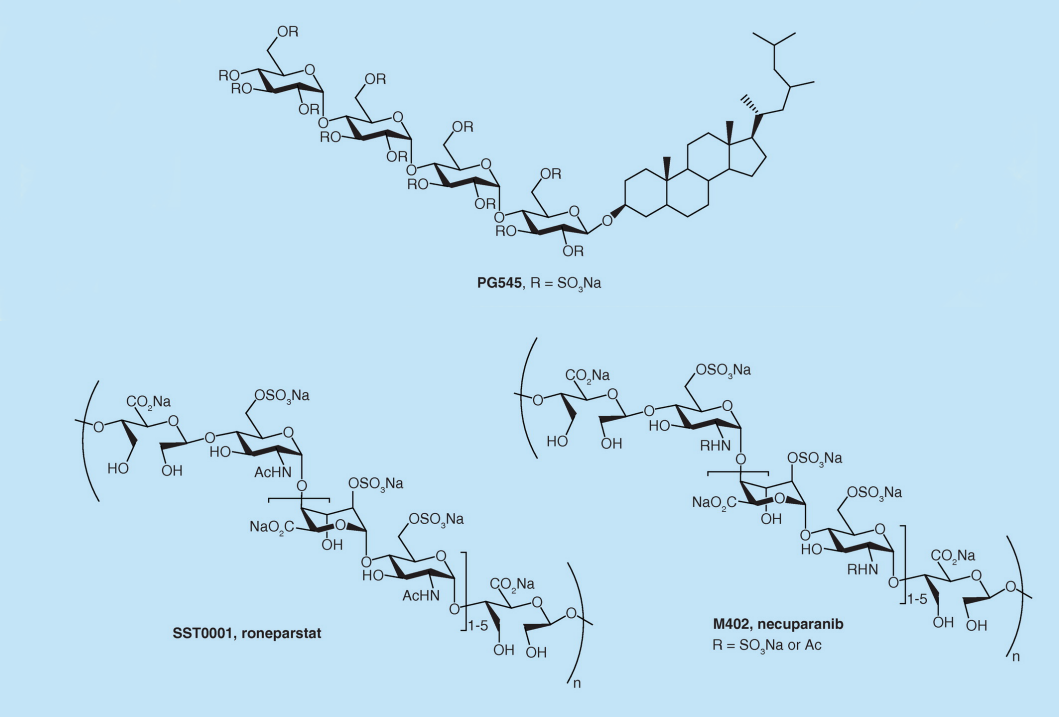

Fig. 7. HPSE inhibitors in clinical trials. From [60].

1.2.3. Heparanase in physiological and pathological condition

In physiological condition HPSE is expressed in few tissues like placenta and keratinocytes, and it seems to be involved in embryotic implantation and development, wound repair, HS turnover, tissue remodelling, immune surveillance and hair growth [84]. In non-cancer cells the expression of HPSE is constitutively inhibited through epigenetic mechanism and through the activity of p53.

In pathological condition (cancer, inflammation, I/R injury and fibrosis) HPSE is upregulated by several factors such as mutated variance of p53, hypoxia, inflammatory cytokines and ROS, hyperglycemia, albuminuria and estrogens [85].

1.2.3.2. Heparanase and inflammation

HPSE is involved in the inflammatory response controlling the release of proinflammatory cytokines (IL-2, IL-8, bFGF, TGF-β), modulating the interaction between leucocytes and vascular endothelium, and favouring leucocytes recruitment, rolling process and extravasation. This leads to the establishment of the innate immune response by the activation of TLRs and NF-kB [60, 86-90]. Moreover, HPSE results to promote monocytes to macrophages activation and to favour the establishment of chronic inflammation [91].

Interestingly, the stimulation of TLRs is among the leading candidate pathways for HPSE-dependent macrophage activation for two main reasons: i) intact extracellular HS inhibits TLR-4 signaling and macrophages activation and so its removal relieves the inhibition; ii) soluble HS released upon HPSE activation can stimulate TLR-4 [92].

As a consequence, HPSE has an essential role in inflammation [93, 94].

1.2.3.3. Heparanase and kidney I/R injury

As demonstrated by our research group, HPSE has a pivotal role in EMT of renal proximal tubular epithelial cells induced by I/R injury [95].

HPSE is crucial to the induction of EMT by FGF-2 and regulates TGF-β-related EMT [96] as well as its production in renal proximal tubular epithelial cells [97, 98]. In fact, diabetic HPSE-ko mice, contrarily to the wild-type (WT), did not show TGF-β increment in renal tissue and did not develop proteinuria, mesangial matrix expansion or tubulo-interstitial fibrosis [99].

Moreover, our research group has recently demonstrated that renal epithelial tubular cells (HK-2) underwent to hypoxia/reoxygenation upregulated HPSE and this enzyme mediated the activation of EMT transcriptional program. This mechanism was inhibited in HPSE-silenced HK-2 and WT cells treated with SST0001 [95]. We confirmed these data in mice overexpressing HPSE (HPA-tg) undergoing I/R injury. They showed more severe renal dysfunction compared to their WT littermates. In particular HPA-tg mice exhibited more tubular dilatation, cell detachment from basement membrane, cast formation and loss of brush

border. In addition, HPA-tg mice displayed higher levels of serum creatinine following renal I/R as compared with WT mice subjected to the same procedure.

Similar results were obtained in a mouse model of AKI. HPA-tg mice display HPSE upregulation along with proinflammatory and pro-fibrotic factors overexpression; a pre-treatment with the HPSE inhibitor PG545 abolished the EMT transcriptional program and cytokines overexpression and improved renal function [100].

HPSE overexpression results also associated with increased macrophages infiltration [95]. Celie et al. showed that, within 24 hours after renal I/R injury, HSPGs in the peri-tubular capillaries were induced to bind L-selectin and MCP-1, facilitating monocytes extravasation [101]. HPSE overexpression, degrading HS and releasing chemokines anchored within ECM and cell surface, sustained continuous activation of kidney damaging macrophages [92].

All these findings indicate that HPSE has a pivotal role in the pathogenesis of renal I/R injury.

2. AIM OF THE STUDY

In this study we investigated the role of HPSE in the recruitment, activation and function of macrophages during I/R injury *in vitro* and in C57BL/6J mice subjected to monolateral I/R injury by vascular clamping.

It is already known that renal epithelial tubular cells can produce a high amount of HPSE after I/R injury contributing to the onset and development of partial EMT. Additionally, HPSE resulted to be involved in the activation of the parenchymal immune inflammatory state modulating monocytes recruitment and activation into macrophages [90-92, 95].

Although macrophages are involved in this mechanism, the complete biological machinery is only partially investigated.

To this purpose we decided to explore: I) the contribution of HPSE on macrophages polarization; II) the effects of HPSE on apoptosis and production of cytokines and DAMPS by I/R injured renal epithelial tubular cells; III) the crosstalk between macrophages and injured renal cells.

3. MATERIAL AND METHODS

3.1. *In Vitro* study

3.1.1. Cell culture and treatments

The following cell lines were employed in the study:
Wild type human renal proximal tubular cells (HK-2) (ATCC® CRL-2190™);
HPSE- silenced HK-2 cells;
Human monocytes (U937).

3.1.1.1. HK-2 cells transfection with HPSE shRNA plasmid

A stable HPSE-silenced HK-2 cell line was obtained by transfection with shRNA plasmid targeting human HPSE (NM_006665) purchased from OriGene (Rockville, MD, USA). Four different shRNAs have been used and shRNA pRS non-effective GFP plasmid (TR30003) was used as negative control.
HK-2 cells were seeded in 6-well plates at a density of $1.5x10^5$ cells per well. When cells reached 70-80% of confluence the medium was replaced with 2 ml of fresh complete growth medium. The transfection mixture was prepared diluting 4 μg of shRNA in 250 μl of M199 medium and 10 μl Lipofectamine™ 2000 (Invitrogen) in 250 μl of M199 medium. After 5 minutes incubation at room temperature the two solutions were combined and incubated for 20 minutes at room temperature. The final transfection mixture was added to each well and mixed gently by rocking the plate back and forth. After 6 hours medium was replaced. Forty-height hours after transfection cells underwent several weeks of selection with 0.75 μg/ml of puromycin (Sigma).

3.1.1.2. HK-2 cells cultures and treatments

HK-2 WT cells were maintained in DMEM-F12 medium with 17.5 mM glucose (EuroClone), supplemented with 10% FBS (Biochrom AG), 2 mM L-glutamine, 100 U/ml penicillin and 100 μg/ml streptomycin. HPSE-silenced HK-2 cells were grown in the same medium of WT cells supplemented with 0.75 μg/ml puromycin.

All cells were grown to sub-confluence and starved for 24 hours in serum-free medium. Then they were seeded in six-well plates and underwent to 24 h hypoxic conditions by the influx of 95% Nitrogen and 5% CO_2 in a hypoxia incubator chamber (STEMCELL) and an indicator test (Sigma Aldrich). The cells were then maintained under normoxic conditions for a reoxygenation phase of 6 hours (gene expression analysis) or 24 hours (protein expression analysis and vitality assay). The cells tested after a complete cycle of hypoxia/reoxygenation are indicated as H/R cells.

Control cells were grown under normoxic conditions for the same time periods. WT HK-2 cells were also treated with or without 200 μg/ml SST0001.

To evaluate the effect of the conditioned medium from M1 or M2 macrophages, WT and HPSE-silenced cells in normoxic condition or after I/R were treated with the conditioned medium of U937 cells polarized to M1 or M2 macrophages (3.1.1.3.).

3.1.1.3. U937 cells

U937 is a human hematopoietic cell line with the properties of immature monocytes. They can be activated by phorbol 12-mystrate 13-acetate (PMA) and polarized to the M1 or M2 phenotype.

3.1.1.3.1. U937 cultures and treatments

U937 cells were cultured in RPMI-1640 medium supplemented with 10% FBS, 100 U/ml penicillin and 100 μg/ml streptomycin. The cells were seeded at a density of 5×10^5 cells/well into six-well plates with RPMI-1640 containing 5% FBS and activated with 100 ng/ml PMA (Sigma) for 48 hours. To induce polarization, cells were incubated with LPS (100 ng/ml) (Santa Cruz) or IL-4 (20 ng/ml) (Preprotec) for 2 hours and then medium was replaced with fresh one for 24 hours. U937 cells were also treated with or without 200 μg/ml SST0001, 1 μg/ml human recombinant heparanase or with the conditioned medium of WT or HPSE-silenced HK-2 cells with or without exposure to H/R.

3.1.2. Biomolecular analysis

3.1.2.1. Cell viability assay

HK-2 cells were plated at a density of 3×10^3 cells/100 µl per well in 96-well plates. The viability of the cells was observed in normoxia (CTR), after 24 hours of hypoxia (H) and after 24 hours of reoxygenation (H/R). Cell viability was determined using a colorimetric method: the CellTiter 96 Aqueous One Solution Cell Proliferation Assay (Promega). Twenty µl of CellTiter 96 Aqueous One Solution Reagent were pipetted into each well, plates were incubated for 1 hour at 37°C and the absorbance were then measured with Microplate Reader Infinite M200PRO (Tecan), OD 490 nm. The experiment was performed twice with six replicates.

3.1.2.2. Analysis of apoptosis by flow-cytometry

The percentage of apoptotic cells was determined under normoxia and H/R conditions in WT and HPSE-silenced cell populations in the presence or absence of SST0001 using the Annexin V-FITC apoptosis detection kit (Immunostep). At the end of the treatments cells were washed twice with PBS and resuspended in 1X Annexin-binding buffer, 10,000 cells/100 µl. Five µl of Annexin V-FITC and 5 µl of propidium iodide (PI) were added at each cells suspension. Cells were incubated at room temperature in the dark for 15 minutes. Then, 400 µl 1X Annexin-binding buffer were added to the samples that were analysed using BD FACSCanto II flow cytometer (BD Biosciences). Results were expressed as the percentage of early apoptotic cells (annexin V^+/PI^-) relative to all cells. The experiment was performed twice in triplicate.

3.1.2.3. Gene expression analysis

Total RNA was extracted from cells using Trizol reagent (Invitrogen). Gene expression was analysed by Real Time PCR.

3.1.2.3.1. RNA extraction

Cells were washed with PBS and 300 µl of Trizol were added, then cells were scraped and Trizol suspension was collected. After 10 seconds of vortex and 10 minutes of incubation at room temperature 60 µl of chloroform were added at the homogenized samples that were vortexed again, incubated 10 minutes at room temperature and then centrifuged at 12,000×g for 15 minutes at 4°C to separate RNA, DNA and proteins. Aqueous phase containing RNA was transferred in a new tube and 150 µl of isopropanol were added. The solution was vortexed and incubated 10 minutes at room temperature followed by centrifugation at 12,000×g for 10 minutes at 4°C to precipitate RNA. The pellet was washed twice with 800 µl 75% ethanol and resuspended in 10 µl of RNAse-free water. RNA was quantified with Nanodrop measuring absorbance at 260 nm and 280 nm. RNA samples were stored at -80°C.

3.1.2.3.2. RNA reverse transcription

Five hundreds ng of total RNA from each sample were reverse-transcribed into cDNA using SuperScript II Reverse Transcriptase (Invitrogen). For a 10 µl reaction volume, in a tube 500 ng of RNA was mixed with 0.5 µl of Random hexamer primer mix (500 µg/ml) (Bioline), 0.5 µl of Deoxynucleotide mix (10 mM) (Sigma) and sterile water up to 6 µl. Mixture was incubated at 65°C for 5 minutes and quick chilled on ice. Content was collected by centrifugation and the following components have been added: 2 µl of 5X First Strand Buffer, 1 µl of 0.1 M DTT, 0.5 µl of SuperScript II RT and 0.5 µl of sterile water. Mixture was incubated at 25°C for 10 minutes, then at 42°C for 50 minutes and at last 70°C for 15 minutes. cDNA was diluted in RNAse-free water up to 4 ng/µl and stored at -20°C.

3.1.2.3.3. Real-time PCR

Real-time PCR was performed on an ABI-Prism 7500 using Power SYBR Green Master Mix 2X (Applied Biosystems) and MicroAmp Optical 384-well reaction plate (Applied Biosystem). In a final volume of 10 µl we used 5 µl of SYBR Green Master Mix, 0.4 µl of forward and reverse primers (5 µM), 2 µl cDNA (4

ng/µl), 2.2 µl of RNAse-free water. Reaction was performed in duplicate with the following real-time PCR parameter:

Polymerase activation	95 degrees – 2 min
	40 cycle:
Denature	95 degrees - 5 sec
Anneal/Extend	60 degrees - 30 sec

The comparative Ct method (ΔΔCt) was used to quantify gene expression and the relative quantification was calculated as $2^{-\Delta\Delta Ct}$. Data were normalized to *GAPDH* expression. Primer sequences are listed in Table 1.

3.1.2.4. Western blotting

Cells were lysed in RIPA buffer (3.30% NaCl 5 M, 2% TRIS 2.5 M, 5% Sodium Deoxycholate 10%, 1% SDS 10%, 1% Triton, pH 8) with Complete Protease Inhibitor Mixture (Sigma-Aldrich). Proteins were quantified with Pierce™ BCA Protein Assay Kit (Thermo Scientific). Briefly, equal amounts of proteins were resolved by 10% SDS-PAGE and electro-transferred to 0.45 µm nitrocellulose membranes (Amersham™ Protran™ Premium 0.45 µm NC). Membranes were placed 2 hours in blocking buffer (TBS-Tween 3% BSA) at room temperature in agitation and then were incubated with primary antibodies diluted in TBS-Tween 0.5% BSA overnight at 4°C. After 3 washing with TBS-Tween, membranes were incubated with a secondary peroxidase-conjugated antibody for 1 hour at room temperature. The signal was detected with SuperSignals West Pico Chemiluminescent substrate solution (Pierce) using Alliance UVitec Mini HD9 Cambrige (Eppendorf). The antibodies are listed in Table 2.

3.1.2.5. Immunofluorescence

HK-2 cells were seeded and treated on Chamber culture slides (Falcon). Cells were fixed in Paraformaldehyde 4% for 10 minutes. After washing with PBS 3 times, cells were covered with quenching solution for 10 minutes and then washed 3 times again with PBS. HK-2 cells were permeabilized with PBS-Triton 0.2% for 10 minutes and washed 3 times. Cells were saturated in PBS containing 1% BSA for 1 hour and then incubated overnight at 4°C with the primary antibody

HMGB1 (GeneTex GTX101277). The cells were washed 3 times with PBS and incubated for 1 hour at room temperature with the secondary antibody. Nuclei were counterstained with Hoechst and slides were mounted with Fluoromount™ (Sigma). Immunofluorescence images were acquired using a Leica TCS SP5 confocal microscope.

3.2. *In Vivo* study

3.2.1. Animal model of kidney ischemia/reperfusion

Wild-type C57BL/6J mice weighing 23–30 g were maintained on a standard diet and water provided ad libitum. The study was carried out according to national guidelines for animal experiments as approved by the local committee for the supervision of animal experiments. We assigned 42 mice randomly to control (N = 14), I/R (N = 14) and I/R+SST0001 (N = 14) groups. In each group, 7 mice were sacrificed 2 days post-I/R and the remaining 7 days post-I/R (Fig. 8). The mice were anesthetized with sodium pentobarbital (50 mg/kg, IP) and placed on temperature-controlled heating table, keeping the body temperature at 37°C. Renal ischemia was induced by clamping the left renal artery for 30 min while the kidney was kept warm and moist. The clamp was then removed, the kidney was observed to confirm the return of blood flow, and the abdominal wall incision was sutured. Control mice underwent the same procedures without clamping. The mice were allowed to recover in a warmed cage. The I/R+SST0001 mice were injected daily (IP) with 0.6 mg SST0001 dissolved in water (Leadiant Biosciences). Control and I/R mice were injected daily with the same volume of water. The mice were killed by cervical dislocation and blood samples were taken at each time point for the measurement of blood urea nitrogen (BUN), creatinine and HPSE activity. One half of the left kidney was snap-frozen in liquid nitrogen and stored at −80°C and the other half was fixed in formalin, embedded in paraffin and used for histological analysis.

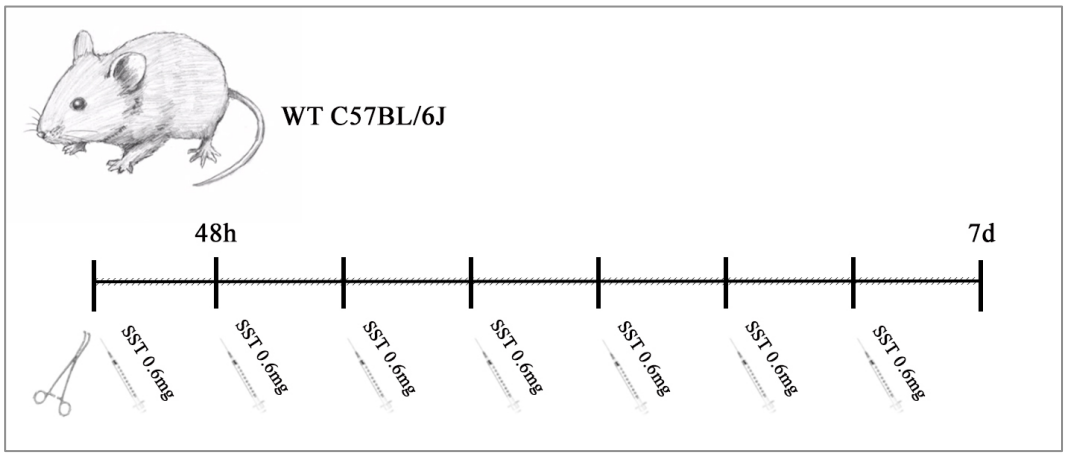

Fig. 8: Male WT C57BL/6J mice were assigned to control (N = 14), I/R (N = 14) and I/R+SST0001 (N = 14) groups. In each group, 7 mice were sacrificed 48 hours post-I/R and the remaining 7 days post-I/R. The I/R+SST0001 mice were injected daily (IP) with 0.6 mg SST0001 dissolved in water. Control and I/R mice were injected daily with the same volume of water.

3.2.2. Biomolecular analysis

3.2.2.1. Gene expression analysis

Total RNA was extracted from frozen renal tissues using Trizol reagent (Invitrogen).

3.2.2.1.1. RNA extraction from renal tissue

A half of frozen renal tissue was homogenized in 1 ml of Trizol. Two hundreds µl of chloroform were added at the homogenized samples that after vortexed were incubated other 10 minutes at room temperature. Samples were then centrifuged at 12000×g for 15 minutes at 4°C to separate RNA, DNA and proteins. Aqueous phase containing RNA was transferred in a new tube and 500 µl of isopropanol were added. The solution was vortexed and incubated 10 minutes at room temperature followed by centrifugation at 12000×g for 10 minutes at 4°C to precipitate RNA. The pellet was washed twice with 1 ml of Ethanol 75% and resuspended in 100 µl of RNAse-free water. RNA was quantified with Nanodrop measuring absorbance at 260 nm and 280 nm. RNA samples were stored at -80°C.

3.2.2.1.2. RNA reverse transcription and Real-time PCR

Five hundred ng of total RNA from each sample were reverse-transcribed into cDNA using SuperScript II Reverse Transcriptase (Invitrogen) following the same protocol used with cells RNA. (3.1.2.3.2.). As the same, the Real-time PCR was performed as reported in 3.1.2.3.3. Primer sequences are listed in Table 1.

3.2.2.2. Western blotting

A half of frozen renal tissue was lysed in 500 µl RIPA buffer (3,30% NaCl 5M, 2% TRIS 2,5M, 5% Sodium Deoxycholate 10%, 1% SDS 10%, 1% Triton, pH 8) with Complete Protease Inhibitor Mixture (Roche). Proteins were quantified with Pierce™ BCA Protein Assay Kit (Thermo Scientific) and western blot analysis were performed as previous described (3.1.2.4.). The antibodies are listed in Table 2.

3.2.3. Histological analysis

3.2.3.1. Tissues inclusion

Tissues were fixed in formalin for 24 hours and were included in paraffin. Fixed kidneys were washed three times with distilled water to remove formalin. Samples were dehydrated through passages in ethanol (Sigma Aldrich) 50%, 70%, 96%, 30 minutes for three times for each ethanol concentration. Samples remained in Ethanol 96% over night at 4°C and then they were put on ethanol 100% for 45 minutes for three times and then in xylene (Sigma Aldrich) for 1 hour for two times. To allow paraffin to replace xylene into the tissues, samples were placed in paraffin Lab-O-Wax (Hysto-Line Laboratories) in a 57°C stove. When xylene evaporated dehydrated kidneys were embedded.

After inclusion, tissues were cut using a microtome to prepare 4 µm sections slides. Paraffin sections were stained with Periodic acid-Shiff (PAS) staining, hematoxylin-eosin and immuofluorescence for histological analysis.

3.2.3.2. PAS staining

To remove paraffin from the sections, slides were placed three times in xylene for 10 minutes and then rehydrated throw passages in ethanol 100% (two times), 96%, 70%, 50%, till distilled water. The staining was performed placing Periodic Acid Solution 1% on slides for 20 minutes at room temperature. After rinse sections in distilled water a drop of Shiff's reagent was put on tissue sections for 1 hour and then slides were rinse in warm tap water for 10 minutes. Nuclei were counterstained with hematoxylin (Sigma) for 10 seconds and then slides were rinse in tap water for 5 minutes. Sections were dehydrated through a series of ascending ethanol prior to being placed in xylene and mounted with Canada balsam (Sigma Aldrich).

3.2.3.3. Hematoxylin-eosin staining

Tissues section were deparaffinized as before (3.2.3.2). To stain nuclei, a drop of hematoxylin (Sigma) was put on each section for 15 seconds and then the stain was fixed in tap water. While to stain cytoplasm slides were covered with a drop of eosin (Sigma-Aldrich) for 20 seconds, the stain was fixed in tap water. Sections were dehydrated through placing them in 50%, 70%, 96%, 100% ethanol to xylene and mounted with Canada balsam (Sigma Aldrich).

3.2.3.4. Immunofluorescence

Tissue sections were deparaffined and antigens were unmasked by heating in a microwave oven in sodium citrate buffer (10 mM sodium citrate, 0.05% Tween-20, pH 6) for 10 minutes and then washed in PBS 10 minutes for three times. The sections were permeabilized with 0.2% Triton X-100 and after three washings were saturated in PBS containing 1% BSA and 0.1% Triton X-100 for 1 hour. Samples were incubated overnight at 4°C with the primary antibodies. The sections were then washed with PBS and incubated for 1 hour at room temperature with the secondary antibodies. Nuclei were counterstained with Hoechst and slides were mounted with Fluoromount™ (Sigma). Immunofluorescence images were acquired using a Leica TCS SP5 confocal microscope.

3.2.3.5. TUNEL assays

Apoptotic cells were detected using the Click-iT TUNEL Alexa Fluor 488 Imaging Assay system (Thermo Fisher Scientific) according to the manufacturer's instructions. The deparaffined tissue sections were fixed in 4% paraformaldehyde for 15 minutes at 37°C. Tissue sections were washed in PBS for 5 minutes and permeabilized with Proteinase K solution for 15 minutes at room temperature. After washing, slides were fixed again in 4% paraformaldehyde for 5 minutes at 37°C, wash twice in PBS and rinse in deionized water. Tissue sections were covered with 100 µl of TdT Reaction Buffer and incubate at 37°C for 10 minutes. TdT Reaction Buffer was removed and replaced by 50 µl of TdT reaction mixture (47 µl TdT Reaction Buffer, 1 µl EdUTP, 2 µl TdT enzyme). Slides were incubated for 1 hour at 37°C and then were rinse in deionized water. Sections were washed 3 times with 3% BSA-0.1% Triton in PBS for 5 minutes and then rinse in PBS. Forty µl of Click-iT Plus TUNEL reaction cocktail (36 µl Click-iT Plus TUNEL Supermix, 4 µl 10X Click-iT Plus TUNEL Reaction buffer additive) were placed on tissue slides for 30 minutes at 37°C, protected from light. Each slide was washed with 3% BSA in PBS and rinsed with PBS. Nuclei were counterstained with Hoechst and slides were mounted with Fluoromount™ (Sigma). Immunofluorescence images were acquired using a Leica TCS SP5 confocal microscope.

3.2.4. Assessment of renal function

To analyze kidney function after I/R injury and SST0001 treatment we performed BUN and creatinine assay in mice plasma. Blood was collected the day of the sacrifice and 20 µl of EDTA 0.5 M pH 8 was added as anticoagulant agent. Blood was then centrifuged at 1500g for 15 minutes at 4°C, and plasma was collected and stored at -20°C.

3.2.4.1. Blood Urea-Nitrogen (BUN) Assay

BUN was measured using a commercial assay kit (Abcam) according to the protocol. Forty-nine µl Urea Buffer Assay have been added to 1 µl of plasma. The

Reaction Mix was then added to each sample and standard solutions. The plate was incubated at 37°C for 60 minutes protected from the light. We measured output on Microplate reader (Infinite M200PRO- Tecan), OD 570 nm.

3.2.4.2. Creatinine assay

Serum Creatinine was detected using Creatinine Assay Kit (Abcam). Thirty µl of Creatinine Detection Reagent was added both to 30 µl of serum sample and standard solutions, and incubated for 30 minutes at room temperature. We measured output on Microplate reader (Infinite M200PRO- Tecan), OD 490 nm.

3.2.4.3. Heparanase Activity Assay

HPSE activity was measured using a standardized enzyme linked immunosorbent assay (ELISA) [27] based on the ability of HPSE to degrade heparan sulfate in Matrigel. Twenty-five µl of matrigel 200 µg/ml (Matrigel™ Basement Membrane Matrix, BD Bioscience) were placed in 96-multiwell plates for ELISA and left to dry at room temperature for 2 hours. The wells were washed with PBST (PBS+0.05% Tween 20). Samples were prepared by mixing 1:4 plasma samples with HPSE buffer (0.1 sodium acetate pH 5, 0.1 mg/ml BSA, 0.01% TritonX-100, protease inhibitor cocktail in presence or absence of low molecular weight heparin (LMWH) (50 µg/ml). The samples were incubated at 37°C overnight. Then, plates were washed with PBST and saturated at room temperature for 2 hours with the blocking buffer (1% BSA, 0.1% Triton X-100 in PBS). Plates were washed and incubated with anti-HS-specific monoclonal antibody (mouse IgM Anti-HS Purif. clone HepSS-1) diluted 1:500 in blocking buffer for 1 hour at room temperature. Wells were washed three times with PBST and incubated with secondary antibody (goat anti mouse IgM HRP-conjugated, Santa Cruz) diluted 1:1000 in blocking buffer for 1 hour at room temperature, under agitation. After three washing with PBST, 50 µl of ABTS [2.2-azino-bis (3-ethylbenzthiazoline-6-sulphonic acid)] chromogenic substrate system for ELISA (Sigma) was added to each well for 15 minutes in the dark. The reaction was blocked with 50 µl of 1% SDS. The absorbance was measured at OD 405 nm with Microplate reader (Infinite

M200PRO-Tecan). The HPSE activity was calculated as the difference between OD 405 nm value with or without LMWH.

3.3. Statistical analysis

Means ± standard deviations (SD) of the real-time PCR data were calculated using Rest2009 software. Differences between treated and untreated cells were compared using a two-tailed Student's *t*-test. A p-value < 0.05 was set as the level of significance for all tests. Gene expression differences were analyzed by linear regression models with groups (control, I/R and I/R+SST at 2 and 7 days post-I/R) as categorical variables. Bonferroni-corrected adjusted means and differences were computed using the control as the referent group. A Bonferroni-corrected p-value < 0.05 was considered as statistically significant.

3.4. Reagents

Product	Company	Catalog number
Acetic acid glacial	CARLO ERBA	401392
β-mercaptoethanol	Sigma-Aldrich	M7154
Bovine serum albumin	Sigma-Aldrich	A2153
ColorBurst Electrophoresis Marker	Sigma-Aldrich	C1992
dNTPs Mix, 10mM Solution	Sigma-Aldrich	D7295
Chloroform	AppliChem	A3633
Eosin Y solution aqueous	Sigma-Aldrich	HT110232
Ethanol	Sigma-Aldrich	2860
Formalin solution, neutral buffered, 10%	Sigma-Aldrich	HT501128
Fluoromount aqueous mounting medium	Sigma-Aldrich	F4680
Hematoxylin solution according to Mayer	Sigma-Aldrich	51275
Hydrochloric acid	Sigma-Aldrich	8256
Glycine	Sigma-Aldrich	G8898
Glycerol	AppliChem	A2926
Isopropanol	Sigma-Aldrich	59304
Lab-O-Wax	Hysto-line	R0040SP
Methanol	Sigma-Aldrich	32213
Methyl blue	Sigma-Aldrich	M5528
Non-fat dry milk	Santa Cruz	sc-2325
NaCl	AppliChem	A2942
SuperSignal West Pico Chemiluminescent substrate solution	Thermo Scientific	PI34080
Protease Inhibitor Cocktail	Sigma-Aldrich	4693116001
Random Examer Primers	BIOLINE	BIO-38028
PBS	Sigma-Aldrich	D5652
SDS	Sigma-Aldrich	L4390
TRIzol Reagent	Invitrogen	15596026
Tri-Sodium citrate dihydrate	AppliChem	A4522
Tris	USB Affymetrix	75825
Triton X-100	Sigma-Aldrich	T8532
Tween-20	Sigma-Aldrich	P2287
Xylene	Sigma-Aldrich	16446

3.5. Enzymes and commercial kits

Product	Company	Catalog number
Annexin V-FITC apoptosis detection kit	immunostep	ANXVF-200T
CellTiter 96 Aqueous One Solution Cell Proliferation Assay	Promega	G3582
Lipofectamine 2000	Invitorgen	11668027
MyTaq DNA Polymerase	BIOLINE	BIO-21105
Pierce™ BCA Protein Assay Kit	Thermo scientific	23225
ABI-Prism SYBR Green Master Mix	Applied Biosystem	4309155
SuperScript II reverse transcriptase	Invitrogen	18064-014

3.6. Cell culture media and reagents

Product	Company	Catalog number
DMEM F-12	Euroclone	ECB7501L
Medium 199	Aurogene	AU-L0355
RNAse-free water USP WFI	Lonza	BE17-724F
RPMI 1640	Euroclone	ECB9006L
shRNA HPSE	OriGene	NM-006665
shRNA pRS	OriGene	TR30003
PBS	Aurogene	AU-L0625
PBS without $Ca2^{+}$ and $Mg2^{+}$	Aurogene	AU-L0615
Puromycin	Sigma-Aldrich	58-58-2
Fetal Bovine Serum	Biochrom AG	S-0415
IL-4	Peprotech	D0815
L-Glutamine 200mM	Euroclone	ECB3000D
LPS	Santa Cruz	sc3535
Penicillin/Streptomycin	Euroclone	ECB3001D
PMA	Sigma-Aldrich	P8139
SST0001	Sigma-Tau	
Trypsin-EDTA 1X in PBS	Euroclone	ECB3052D
Trypan Blue	Euroclone	ECM0990D

3.7. Primers and antibody tables

	Gene	forward	reverse	amplicon (bp)
human	GAPDH	ACACCCACTCCTCCACCTTT	TCCACCACCCTGTTGCTGTA	112
	αSMA	GAAGAAGAGGACAGCACTG	TCCCATTCCCACCATCAC	143
	CASP1	TGCCTGTTCCTGTGATGTGG	TGTCCTGGGAAGAGGTAGAAACATC	132
	HPSE	ATTTGAATGGACGGACTGC	GTTTCTCCTAACCAGACCTTC	136
	IL8	ACCACCGGAAGGAACCATCTCACT	CTTGGCAAAACTGCACCTTCACAC	114
	IL10	GCTGGAGGACTTTAAGGGTTACCT	CTTGATGTCTGGGTCTTGGTTCT	109
	IL6	GCCCACCGGGAACGAAAGAGA	GACCGAAGGCGCTTGTGGAGAAG	81
	IL1β	CCTGTCCTGCGTGTTGAAAGA	GGGAACTGGGCAGACTCAAA	150
	iNOS	AGGAGATGCTGAACTACG	GGATGGTGACTCTGACTC	192
	MR	CGAGGAAGAGGTTCGGTTCACC	GCAATCCCGGTTCTCATGGC	84
	TLR2	ATCCTCCAATCAGGCTTCTCT	ACACCTCTGTAGGTCACTGTTG	163
	TLR4	CATCATCCTCACTGCTTCTGT	CATCATCCTCACTGCTTCTGT	106
	TNFα	CCCCAGGGACCTCTCTCTAATC	GGTTTGCTACAACATGGGCTACA	98
mouse	GAPDH	GGCAAATTCAACGGCACAGT	GTCTCGCTCCTGGAAGATGG	84
	Arg-1	TGGCTTGCGAGACGTAGAC	GCTCAGGTGAATCGGCCTTTT	160
	CASP1	CGTCTTGCCCTCATTATC	CACCTCTTTCACCATCTC	159
	HPSE	CAAGAACAGCACCTACTCAAG	AGCAGTAGTCAAGGAGAAGC	155
	IL10	ATACTGCTAACCGACTCCT	ATGGCCTTGTAGACACCT	284
	IL6	CTGCAAGAGACTTCCATCCAGTT	GAAGTAGGGAAGGCCGTGG	70
	IL1β	TGTTTTCCTCCTTGCCTCT	TGCCTAATGTCCCCTTGA	100
	iNOS	CAGCTGGGCTGTACAAACCTT	CATTGGAAGTGAAGCGTTTCG	95
	MR	CAAGGAAGGTTGGCATTTGT	CCTTTCAGTCCTTTGCAAGC	111
	TLR2	AGACGCTGGAGGTGTTGG	AACGAAGCATCTGGGAGT	121
	TLR4	AGAATGAGGACTGGGTGA	TGTAGTGAAGGCAGAGGT	81
	TNFα	CATCTTCTCAAAATTCGAGTGACAA	TGGGAGTAGACAAGGTACAACCC	175

TABLE 1: Primer used to perform Real-time PCR analysis.

		application	catalogue number	brand
primary antibodies	GAPDH	WB	sc-25778	Santa Cruz Biotehnology
	iNOS	WB, IF	NB300-605	Novus
	Arg-1	WB, IF	sc-18351	Santa Cruz Biotehnology
	IL1β	WB	sc-7884	Santa Cruz Biotehnology
	HMGB1	IF	GTX101277	GeneTex
	Caspase-1	WB	sc-515	Santa Cruz Biotehnology
	HPSE	WB, IF	sc-225826	Santa Cruz Biotehnology
	F4/80	IF	ab186073	abcam
	DC68	WB	14-0681	eBioscience
	TNFα	WB	sc-1350	Santa Cruz Biotehnology
secondary antibodies	anti-rabbit HRP	WB	sc-2004	Santa Cruz Biotehnology
	anti-mouse HRP	WB	sc-2005	Santa Cruz Biotehnology
	anti-rat HRP	WB	ab97057	abcam
	anri-chiken A546	IF	A-11040	ThermoFisher
	anti-goat A663	IF	A-21082	ThermoFisher
	anti-rabbit A488	IF	A-11034	ThermoFisher

TABLE 2: Primary and secondary antibody used to perform western blot and immunofluorescence.

4. RESULTS

4.1. *In Vitro* results

4.1.1. HPSE promotes monocytes activation

To assess the role of HPSE in monocytes activation, U937 cells were treated with PMA in combination or not with HPSE for 48 hours. Then, the mRNA levels of TNF-α and IL-1β (two main cytokines expressed form activated macrophages [102]) were measured by Real–Time PCR (Fig. 9A-B).

As expected PMA-treated U937 cells showed upregulation of both genes compared to control cells. The co-administration of PMA and HPSE exacerbates the expression of TNF-α and IL-1β, thus confirming the pivotal role of HPSE in macrophages activation [103].

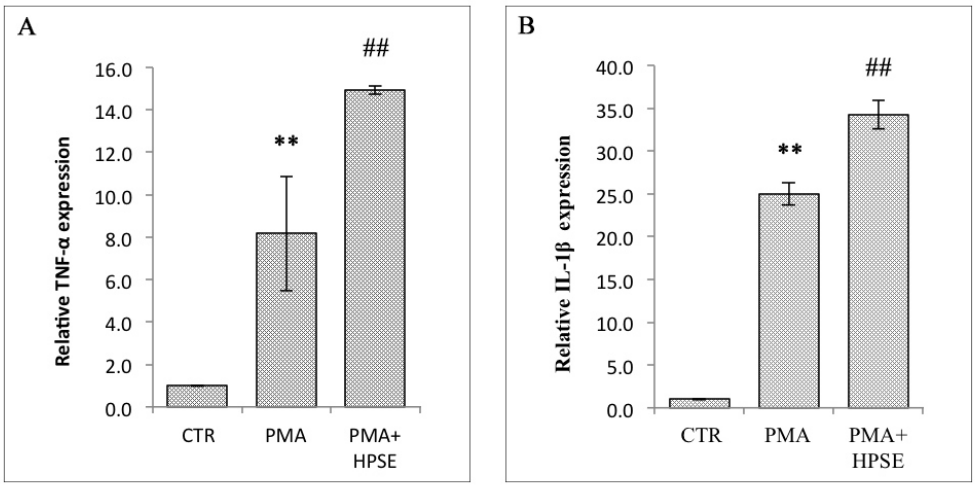

Fig. 9: U937 activation by HPSE. U937 cells exposed or not to PMA were also treated with 1 µg/ml heparanase. The expression of A) TNF-α and B) IL-1β was evaluated by real-time PCR. Data were normalized to GAPDH expression. Mean ± SD (error bars) of two separate experiments performed in triplicate: **p<0.001 vs. CTR; # #p<0.001 vs PMA.

4.1.2. HPSE induces M1 proinflammatory macrophage polarization

U937 cells activated with PMA for 48 hours were treated with HPSE or with the HPSE inhibitor SST0001. Moreover, these treatments were applied in co-administration with LPS (M1 phenotype inducer) or IL-4 (M2 phenotype inducer).

The expression of the proinflammatory markers TNF-α, IL-6, iNOS and IL-1β were measured in activated and LPS-polarized U937 cells by real-time PCR and western blot.

HPSE induced the upregulation of TNF-α, IL-6, iNOS and IL-1β; the co-administration of LPS exacerbated this effect. The inhibition of HPSE with SST0001 suppressed the expression of these proinflammatory genes, especially in LPS-treated cells (Fig. 10A-D). Protein analysis confirmed gene expression results for iNOS and IL-1β (Fig. 10E).

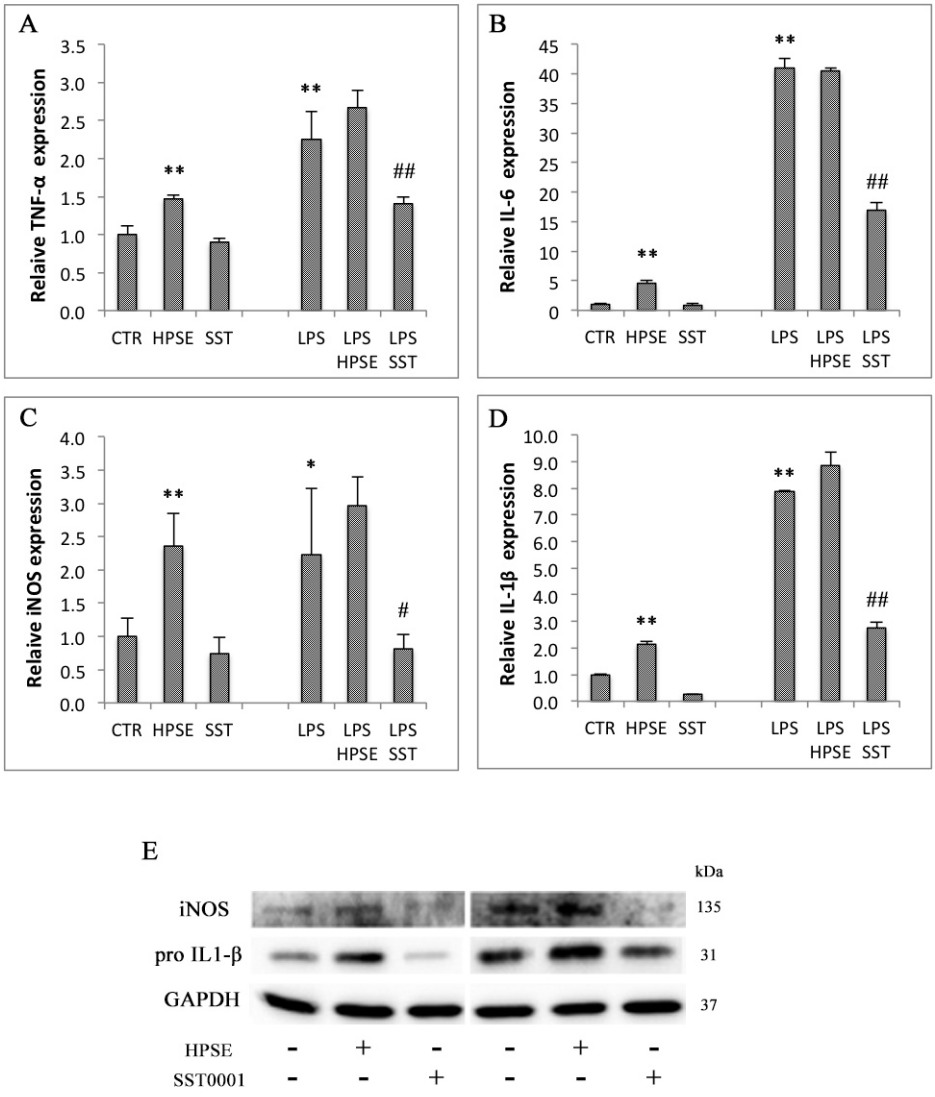

Fig. 10: Gene and protein expression of proinflammatory cytokines during M1 macrophage polarization. M1-associated gene expression of TNF-α (A), IL-6 (B), iNOS (C) and IL-1β (D) was evaluated by real-time PCR on PMA-activated U937 cells exposed to LPS in presence or absence of 1 μg/ml HPSE or 200 μg/ml SST0001. Data were normalized to GAPDH expression. Means ± SD (error bars) of two separate experiments performed in triplicate. **$p<0.001$, *$p<0.05$ vs. CTR, $^{\#\#}p<0.001$, $^{\#}p<0.05$ vs. LPS. E) Protein levels of iNOS and IL-1β evaluated by Western blot. GAPDH was included as loading control.

In addition, for the same cell treatment, we analysed the expression of TLR-2 and TLR-4, well-known components of M1 program [104].

Our results showed that LPS increased only the expression of TLR-2, as previously reported [105], while HPSE up-regulated the expression of both TLR-2 and -4 and this effect was suppressed by SST0001 (Fig. 11A-B). These results revealed that HPSE facilitated the polarization of macrophages into M1 phenotype favouring the activation of TLRs pathway and the production of proinflammatory cytokines.

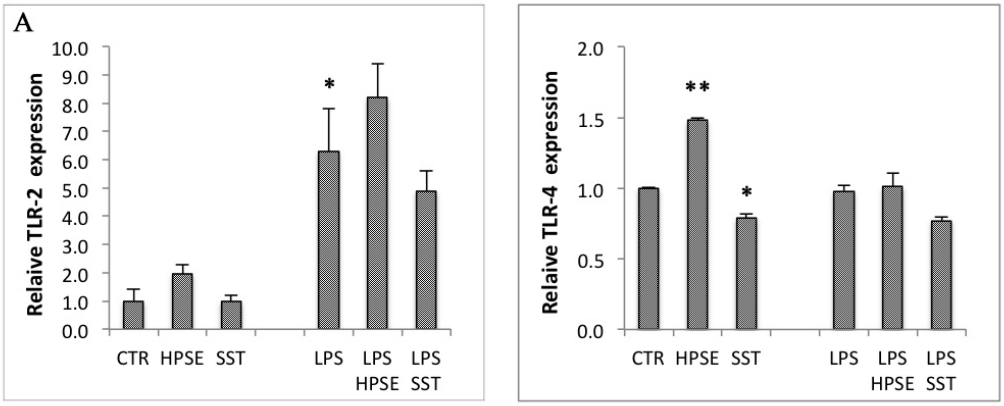

Fig. 11: TLR-2 and -4 gene expressions during M1 macrophage polarization. PMA-activated U937 cells were exposed to LPS in presence or absence of 200 µg/ml SST0001 or 1 µg/ml HPSE. Expression of TLR-2 (A) and TLR-4 (B) was evaluated by real-time PCR. Data were normalized to GAPDH expression. Means ± SD (error bars) of two separate experiments performed in triplicate. **p<0.001, *p<0.05 vs. CTR.

The effects of HPSE on M2 macrophages polarization were investigated measuring the expression of the M2 markers (MR and IL-10) in activated and IL-4 polarized U937 cells by real-time PCR.

HPSE and its inhibitor did not affect the expression of MR while the administration of IL-4, used as a positive control, increased its expression (Fig. 12A). SST0001 reduced the basal expression of IL-10, whereas it did not have any effect on IL-4 treated cells. HPSE significantly reduced IL-10 expression in IL-4 stimulated U937 cells (Fig. 12B).

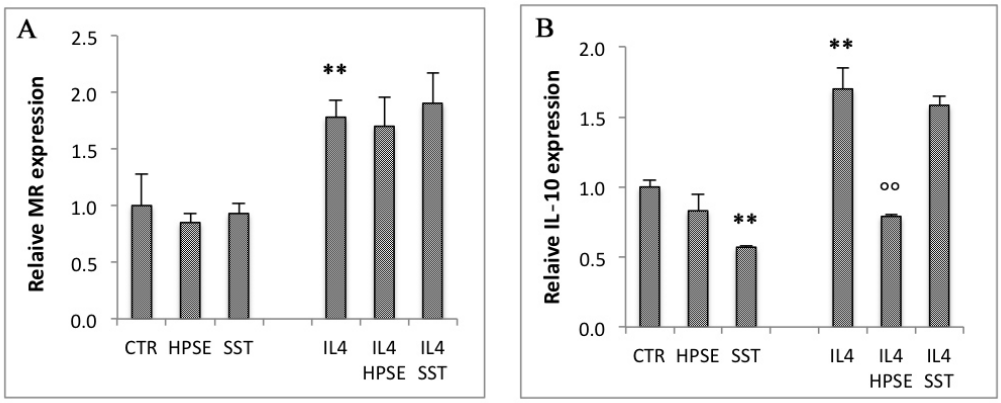

Fig. 12: Anti-inflammatory cytokine gene expression during M2 macrophage polarization. M2-associated gene MR (A), and IL-10 (B) expression was evaluated by real-time PCR on PMA-activated U937 cells exposed to IL-4 in presence or absence of 1 µg/ml HPSE or 200 µg/ml SST0001. Data were normalized to GAPDH expression. Means ± SD (error bars) of 2 separate experiments performed in triplicate. **p<0.001 vs. CTR, °°p<0.001 vs. IL-4.

4.1.3. HPSE modulates the expression of TLRs and DAMPs and promotes apoptosis in renal epithelial tubular cells

The expression of TLRs can be induced also in epithelial tubular cells following H/R, thus promoting the release of proinflammatory cytokines [106].
To better understand the role of HPSE in this context we measured the expression of TLR-2 and -4, the nuclear-cytoplasmic translocation of the High Mobility Group Box Protein 1 (HMGB1) protein and the frequency of apoptosis in WT and HPSE-silenced HK-2 cells, as well as in WT cells treated with SST0001. HMGB1 is a nuclear protein that acts as a DAMP when it translocates from the nucleus into the cytoplasm and then is released into the extracellular fluids [107].
In WT HK-2 cells H/R up-regulated the expression of both TLR-2 and -4, while their expression in HPSE-silenced and in cells treated with the HPSE inhibitor did not change (Fig. 13A-B). The upregulation of TLRs and their activation is consequence of the release of DAMPs such as HMGB1 from injured cells.
By immunofluorescence we detected the translocation of HMGB1 into WT HK-2 cells cytoplasm after H/R, whereas it remained in the nucleus when HPSE was silenced or inhibited (Fig. 13C).
The analysis on cells viability after H/R injury underlined the involvement of HPSE in the development of kidney I/R damage. In fact, HK-2 cells viability was reduced after H/R and the amount of apoptosis was increased, but these effects were inhibited by the administration of SST0001 or the HPSE gene silencing (Fig. 13D-E).

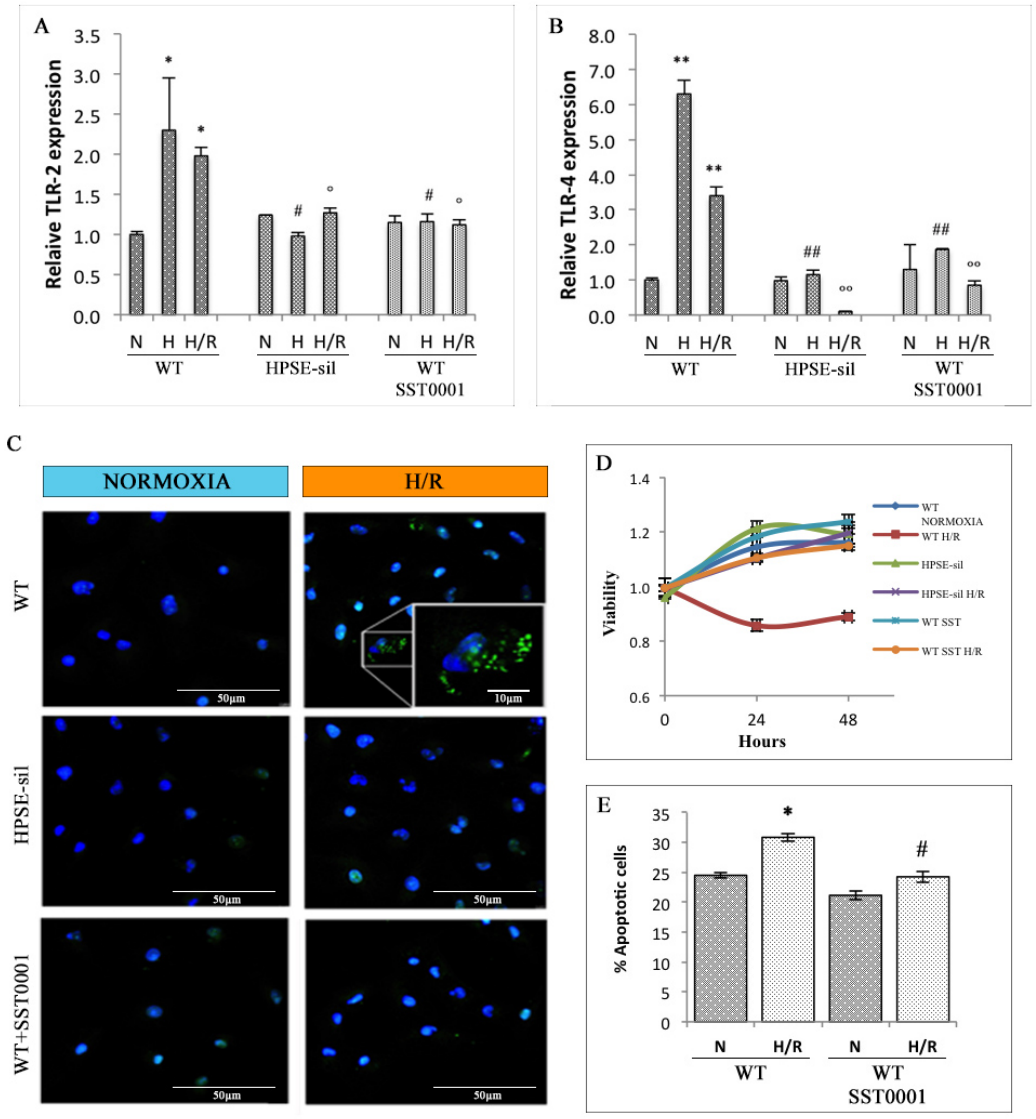

Fig. 13: TLR expression, DAMP production and cell viability and apoptosis, in H/R-injured tubular epithelial cells. WT and HPSE-silenced HK-2 cells were exposed to H/R, and WT cells were also treated or not with 200 µg/ml SST0001. Expression of TLR-2 (A) and TLR-4 (B) was evaluated by real-time PCR. Data were normalized to GAPDH expression. Means ± SD (error bars) of two separate experiments performed in triplicate. **p<0.001, *p<0.05 vs. wild-type N, ##p<0.001, #p<0.05 vs. wild-type H, °°p<0.001, °p<0.05 vs. wild-type H/R. C) Representative images of one of two immunostaining experiments for HMGB1 (green) in WT and HPSE-silenced cells with or without SST0001. Nuclei were counterstained with Hoechst dye (blue). D) Cell viability was measured by MTS assay 24 and 48 hours after H/R. Error bands represent SD from two experiments performed with 6 replicates. E) Evaluation of cell death by apoptosis using annexin V–FITC/PI staining. Percentage of apoptotic cells is shown in bar diagram as mean ± SD from two experiments in duplicate. *p<0.05 vs. wild-type N, #p<0.05 vs. wild-type H/R. N, normoxia; H, hypoxia; H/R, hypoxia/reoxygenation.

4.1.4. HPSE regulates the production of proinflammatory cytokines by HK-2 cells

To assess the potential role of HPSE in the production of proinflammatory cytokines by HK-2 cells we measured the gene expression of TNF-α, IL-6, IL-8, IL-1β and CASP-1, as well as IL-1β and CASP-1 protein level in our *in vitro* model.

H/R strongly increased gene expression of the five proinflammatory cytokines (Fig. 14A-E) and the protein level of IL-1β and CASP-1 (Fig. 14F) in WT HK2 cell but the lack of HPSE induced through inhibition or silencing, inhibited this effect.

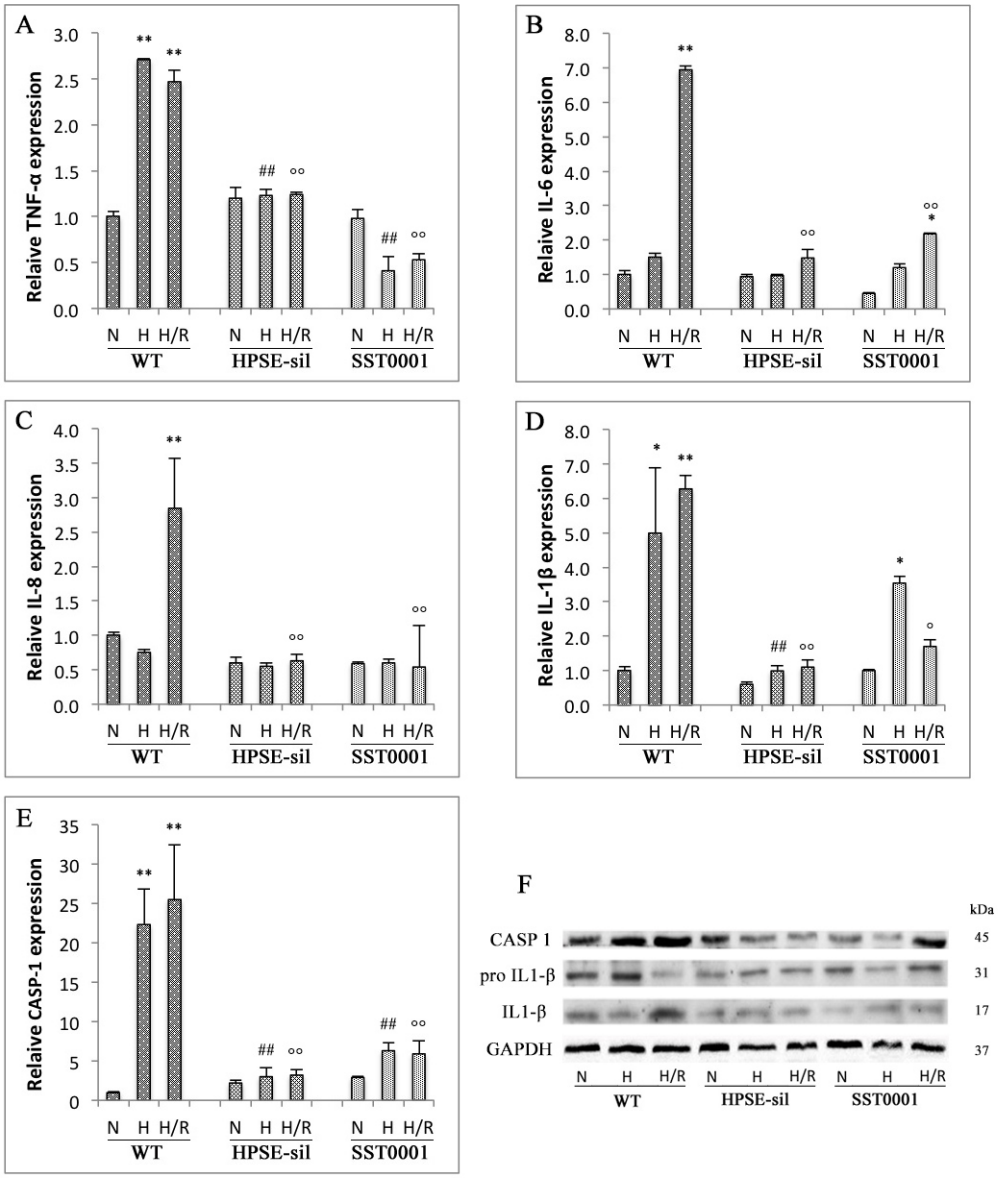

Fig. 14: Proinflammatory cytokines in HK2 cells undergoing H/R. Expression of TNF-α (A), IL-6 (B), IL-8 (C), IL-1β (D), and Capase-1 (E) was evaluated by real-time PCR. Data were normalized to GAPDH expression. Means ± SD (error bars) of two separate experiments performed in triplicate. **p<0.001, *p<0.05 vs. wild-type N, ##p<0.001, #p<0.05 vs. wild-type H, °°p<0.001, °p<0.05 vs. wild-type H/R. F) Caspase-1 and IL-1β protein levels were evaluated by Western blot analysis. GAPDH was included as loading control. N, normoxia; H, hypoxia; H/R, hypoxia/reoxygenation.

4.1.5. HPSE regulates macrophages polarization induced by conditioned medium from HK2 cells injured by H/R

DAMPs and cytokines produced by renal tubular epithelial cells together with the upregulation of HPSE after H/R may promote M1 macrophages polarization [95]. We treated activated U937 cells with the conditioned medium from WT and HPSE-silenced HK-2 cells exposed to H/R and then we analysed the genes expression of M1 (TNF-α, IL-1β, iNOS) and M2 (IL-10, MR) markers.

The conditioned medium from WT tubular cells, collected immediately after hypoxia, stimulated the expression of proinflammatory cytokines from PMA-activated U937, while the conditioned medium from silenced HK-2 cells slightly decreased the expression of these cytokines, in particular IL-1β (Fig. 15A-C). Western blot confirmed gene expression analysis for IL-1β and iNOS and showed the same trend for CASP-1 (Fig. 15D).

On the contrary, the conditioned medium from WT tubular cells exposed to H/R down-regulated the expression of the anti-inflammatory cytokine IL-10 in U937-activated cells, whereas the medium from HPSE-silenced HK-2 cells did not have any effect. MR expression was not modulated by HK-2 conditioned media (Fig. 15E-F).

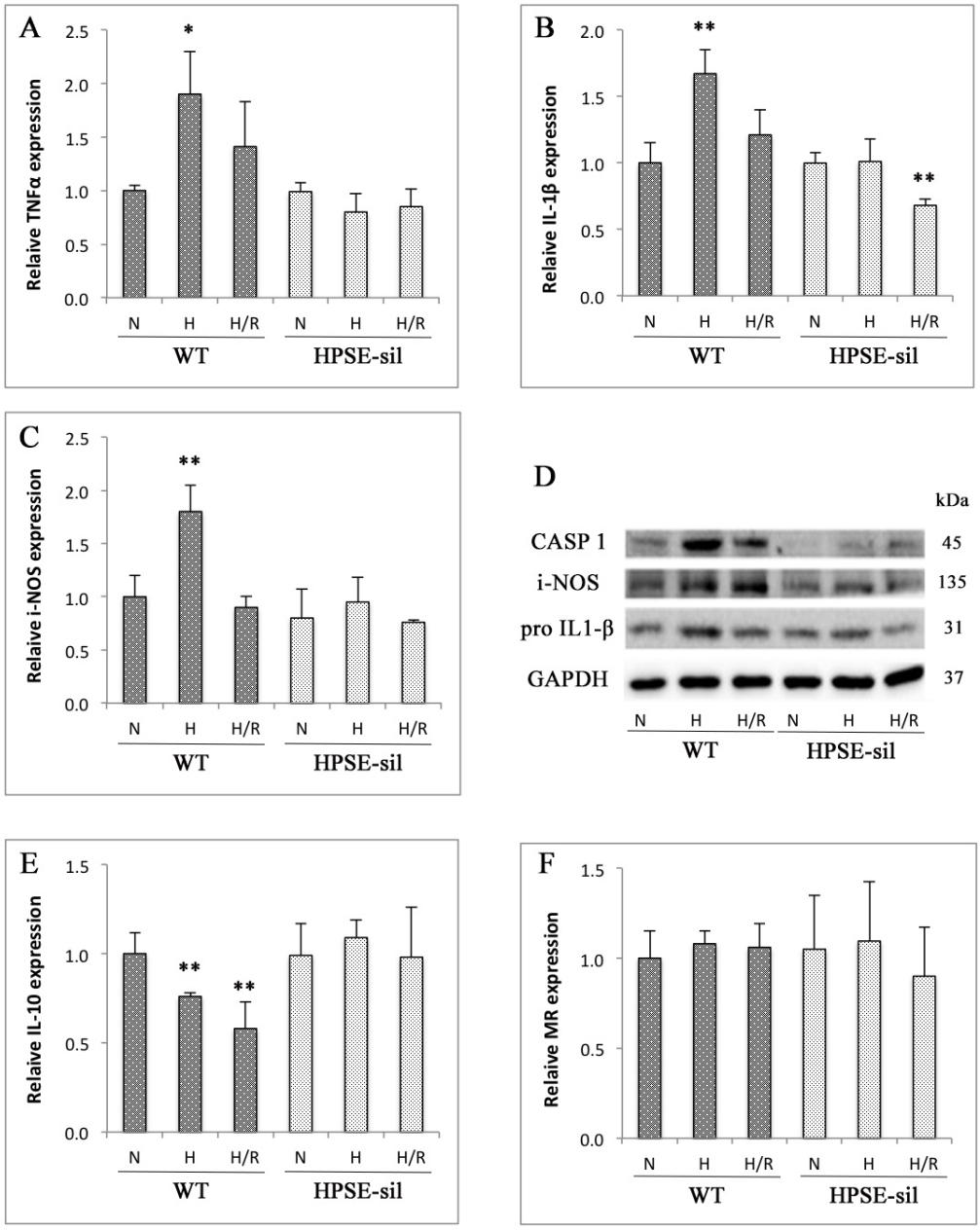

Fig. 15: Expression of cytokines by PMA-activated U937 cells treated with the conditioned media from tubular cells exposed to H/R. PMA-activated U937 cells were exposed to conditioned mediua from WT and HPSE-silenced HK-2 cells collected in normoxia, after ischemia, and after reoxygenation. Expression of TNF-α (A), IL-1β (B), iNOS (C), MR (E), and IL-10 (F) was evaluated by real-time PCR. Data were normalized to GAPDH expression. Means ± SD (error bars) of two separate experiments performed in triplicate. **p<0.001, *p<0.05 vs. WT normoxia. D) CASP-1, iNOS, and IL-1β protein levels evaluated by Western blot analysis. GAPDH was included as loading control.

4.1.6. Conditioned medium from M1 polarized macrophages induced partial EMT program in renal epithelial tubular cells

The *in vitro* profibrotic effects of polarized macrophages on renal tubular epithelial cells were investigated by measuring the expression of 4 well-known EMT markers (α-SMA, VIM, FN, and SNAIL) in wild-type and HPSE-silenced HK-2 cells maintained under normoxic conditions or exposed to H/R. In order to better define which specific pool of macrophages was able to induce a partial EMT in renal epithelial tubular cells, we treated wild-type HK-2 cells with conditioned medium of M1 or M2 macrophages under normoxic conditions or exposed to H/R. The same medium was added to HPSE-silenced tubular cells to assess whether the lack of HPSE could protect these cells from EMT.

Conditioned medium from M1-polarized U937 cells caused the strong upregulation of all the four EMT markers in WT HK-2 cells undergoing H/R. M2-conditioned medium had no effects on WT HK-2 cells under normoxic condition but significantly reduced α-SMA, FN and SNAIL expression compared to WT tubular cells exposed to H/R (Fig. 16A-D).

M1-conditioned medium had no effect in HK-2 cells under normoxic conditions while after H/R there is a mild upregulation of α-SMA, VIM and FN (Fig. 16A-D).

The treatment with the conditioned medium from M2 macrophages had no effects on HPSE-silenced HK-2 cells either under normoxic condition or after H/R (Fig. 16A-D).

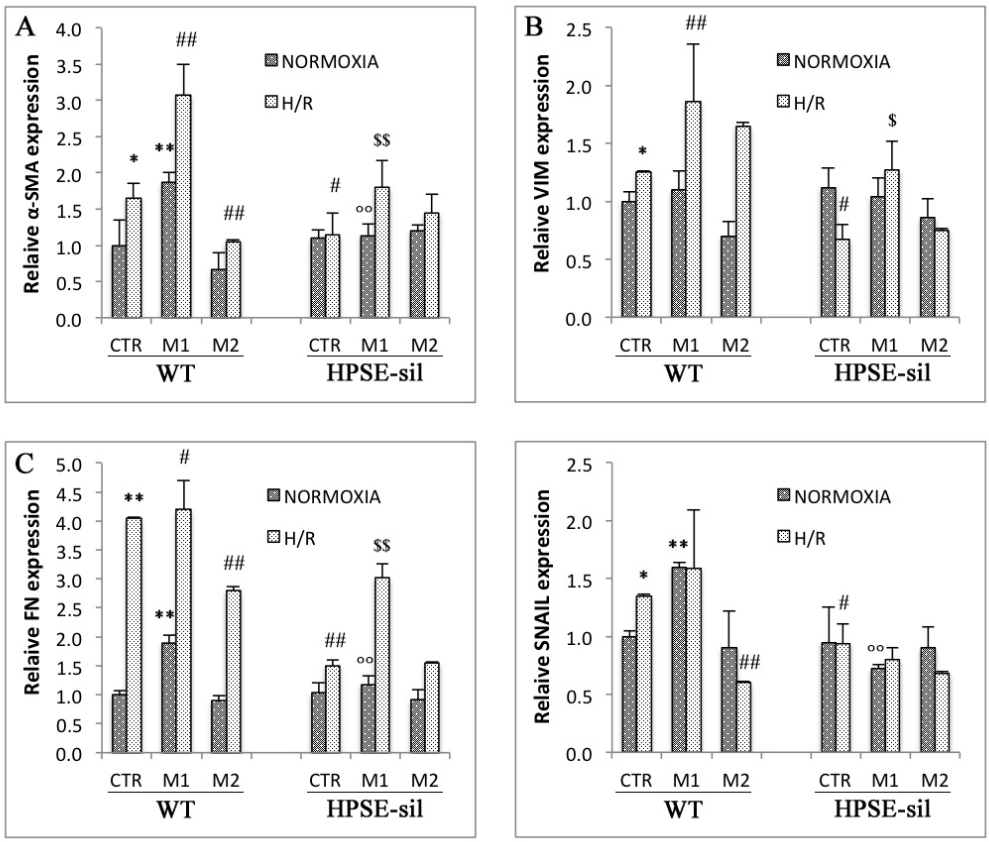

Fig. 16: mRNA levels of EMT markers in HK-2 cells treated with conditioned media form M1 and M2 macrophages. WT and HPSE-silenced (HPSE-sil) HK-2 cells were exposed to H/R, and after hypoxia HK-2 culture medium was replaced with conditioned medium collected from M1- and M2-polarized U937 cells. Expression of a-SMA (G), VIM (H), FN (I), and SNAIL (J) was evaluated by real-time PCR. Data were normalized to GAPDH expression. Means ± SD (error bars) of two separate experiments performed in triplicate. *p<0.05, **p<001 vs. WT CTR/normoxic, $^{\#}$p<0.05, $^{\#\#}$p<0.001 vs. WT CTR H/R, °°p<0.001 vs. WT M1 normoxia, §p<0.05, §§p<0.001 vs. WT M1 H/R. CTR, control.

Because of IL-1β is the most abundant cytokine produces by M1 macrophages and able to induce EMT in renal tubular epithelial cells [108], we measured the level of IL-1β released in the conditioned medium of PMA-activated U937 cells treated with LPS or IL-4.

Both precursor and active form of IL-1β were detected in the conditioned medium from M1 but not M2 macrophages. In addition, pre-treatment with HPSE increased the release of IL-1β in LPS-stimulated cells while in IL-4-polarized U937 only a mild presence of IL-1β precursor was detected. SST0001 reduced the expression of this cytokine in both treatments (Fig. 17).

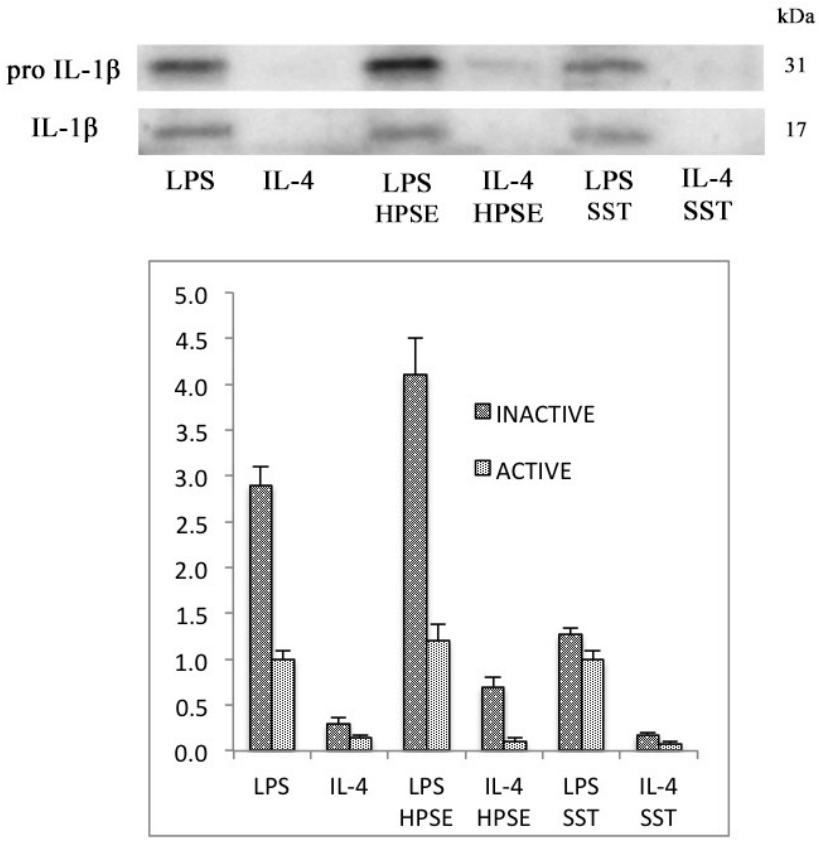

Fig. 17: IL-1β released by U937 cells. The release of IL-1β protein in conditioned medium of PMA-activated U937 cells exposed to LPS or IL-4 in the presence or absence of 200 µg/ml SST0001 or 1 µg/ml HPSE was evaluated by western blot. Histogram represents quantification of active (17 kDa) and inactive (precursor, 31 kDa) IL-1β protein.

4.2. *In Vivo* results

To confirm the results obtained *in vitro* we used an animal model of unilateral kidney I/R injury. We induced I/R in 2 groups of mice by clamping one of the renal arteries for 30 min, with one group receiving no treatment and the other treated with SST0001. The mice were humanely killed 2 or 7 d after I/R.

4.2.1. I/R induces HPSE expression in injured kidney

Gene expression, protein analysis and immunofluorescence staining of the total renal parenchyma revealed the upregulation of HPSE 7 days after ischemic injury; the administration of SST0001 significantly reduced the expression of the enzyme at both time points (Fig. 18A-D). Immunofluorescence showed that HPSE was expressed not only in the glomeruli and tubular cells (white arrowhead) but also in the interstitial cells (red arrowhead) (Fig. 18A). HPSE activity in plasma increased after 7 days in the untreated mice while decreased in mice injected with SST0001 (Fig. 18C).

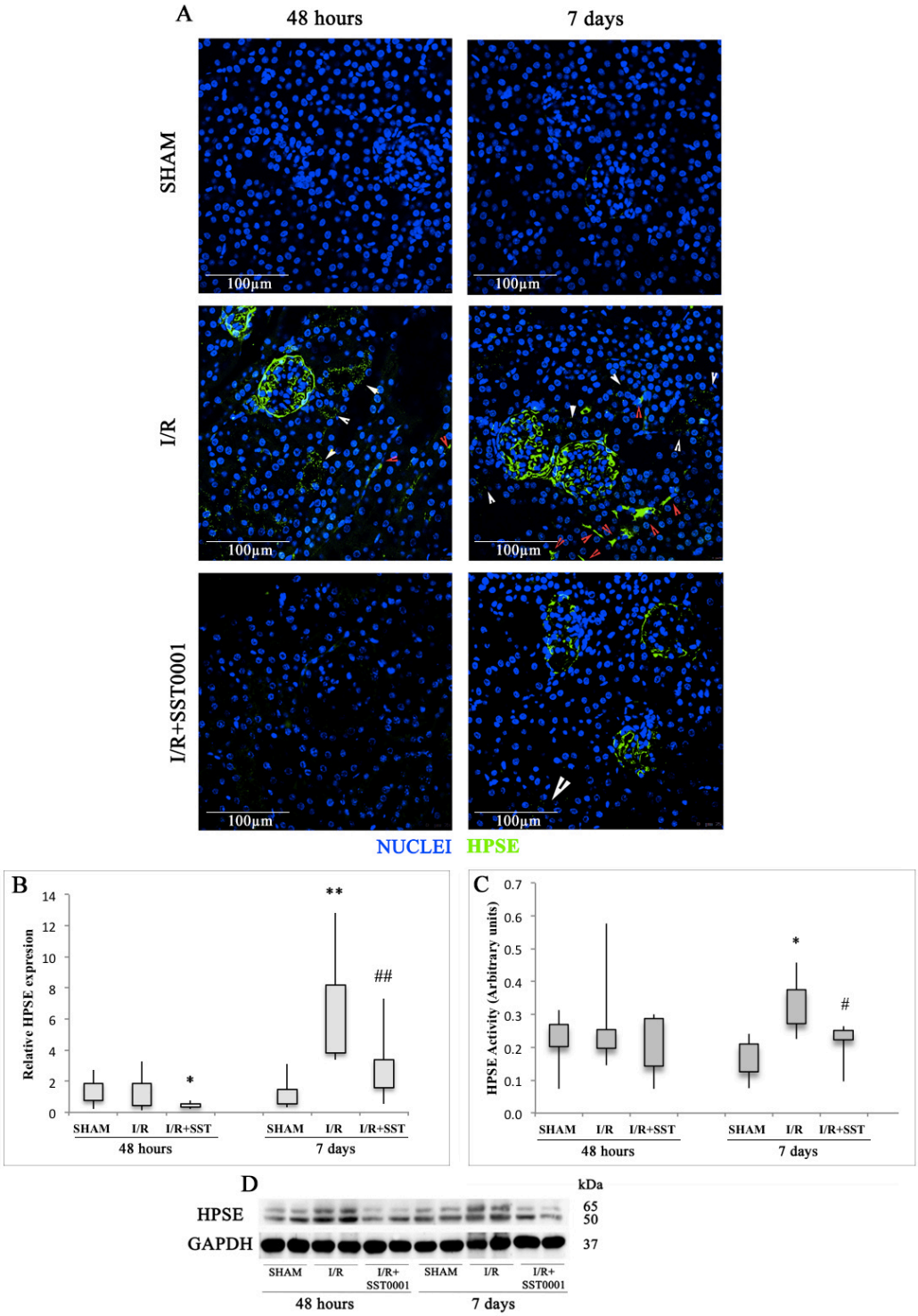

Fig. 18: *In vivo* HPSE expression and activity induced by monolateral renal I/R. A) Representative immunofluorescence staining for HPSE (green) in cortical renal tissues of mice 48 hours and 7 days after sham operation or I/R kidney injury. Nuclei were counterstained in blue. White arrowheads indicate HPSE expression in glomeruli and tubular cells; red arrowheads indicate HPSE expression in interstitial cells. B) Box plot representing relative gene expression of HPSE evaluated by real-time PCR in renal tissue (n = 7). Results were normalized to GAPDH

expression. Graph represents two separate experiments performed in triplicate. C) Box plot representing HPSE activity evaluated by ELISA in plasma samples collected from killed mice. Graph shows two separate experiments performed in triplicate. *$p<0.05$, **$p<0.001$ vs. sham-treated animals. $^{\#}p<0.05$ vs. I/R. D) HPSE protein levels measured by Western blot analysis in randomly selected samples of total kidney lysates. GAPDH was used as loading control.

4.2.2. HPSE promotes *in vivo* macrophages infiltration/polarization towards M1 phenotype and inflammation after I/R in kidney

As expected, renal immunofluorescence staining revealed macrophages infiltration ($F4/80^+$ cells) in untreated mice 2 and 7 days after I/R injury (Fig. 19A-B). Interestingly, in this group of mice 2 days after the injury all infiltrating macrophages resulted positive for iNOS (M1 marker) and completely negative for Arg1 (M2 marker) (Fig. 19A), while 7 days after, besides a prolonged iNOS upregulation, there was an increased number or $Arg1^+$ cells (Fig. 19B).
On the contrary, mice treated with SST0001 exhibited a lower number of $F4/80^+$ cells at both time points and surprisingly most of them were double-positive for iNOS and Arg1 (Fig. 19A-B).

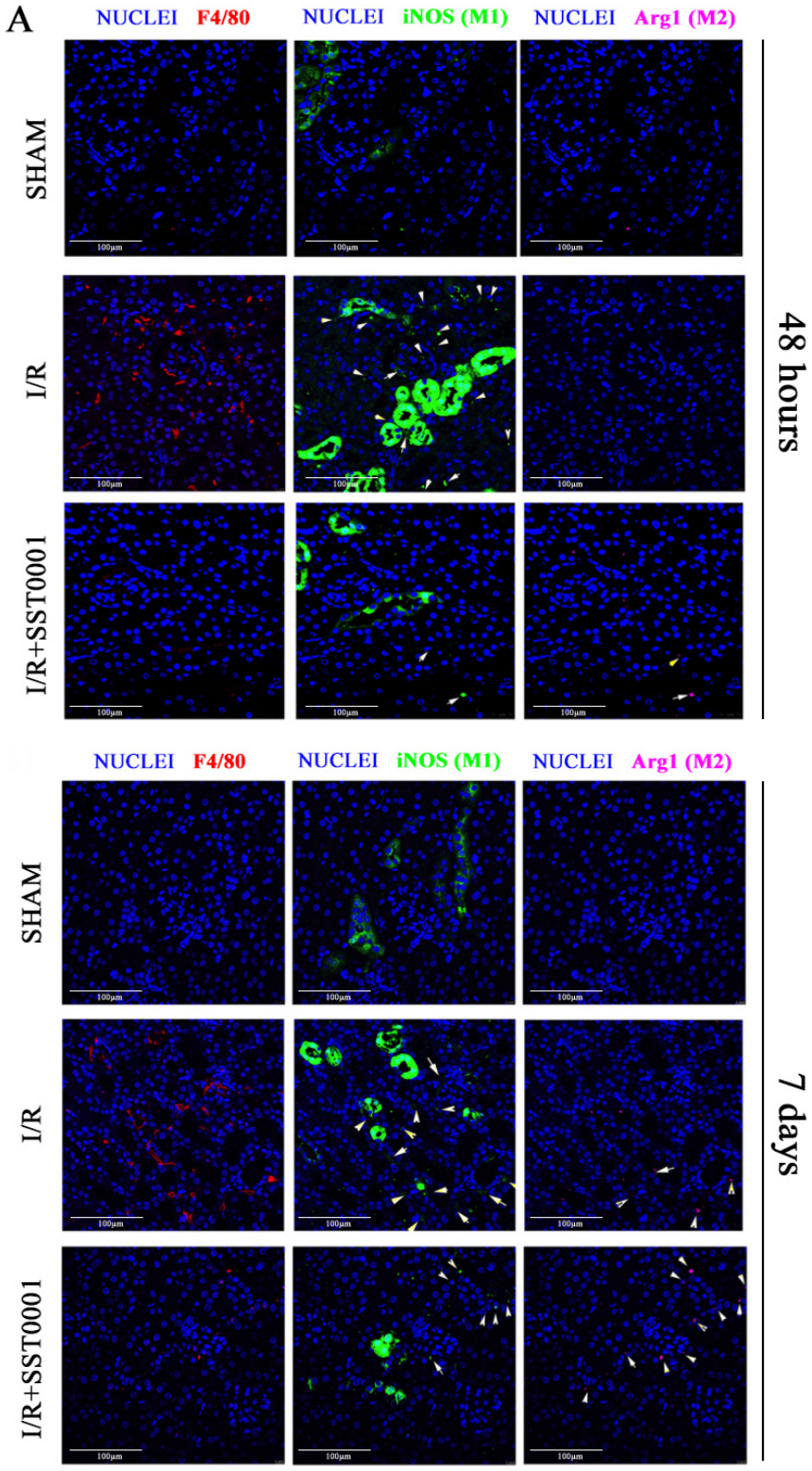

Fig. 19: Macrophages polarization *in vivo*. Representative immunofluorescence staining for F4/80 (red), iNOS (green), and Arg1 (pink) was performed in renal tissue 48 hours (A) and 7 days (B) after I/R. Macrophages are highlighted with arrowheads.

Gene expression analysis performed on the total renal parenchyma supported these evidences. Infact, iNOS was up-regulated 48 hours and 7 days after I/R in untreated mice whereas the treatment with SST0001 lowered its expression to basal level (Fig. 20A). Furthermore, gene expression confirmed the increased of M2 markers expression 7 days after I/R; SST0001 treatment did not affect M2 markers expression (Fig. 20B-C). These findings were sustained by protein analysis that showed a lower abundance of CD68 (macrophages marker) in kidney of SST0001-treated mice at both time points, while Arg1 expression remained unchanged (Fig. 20D).

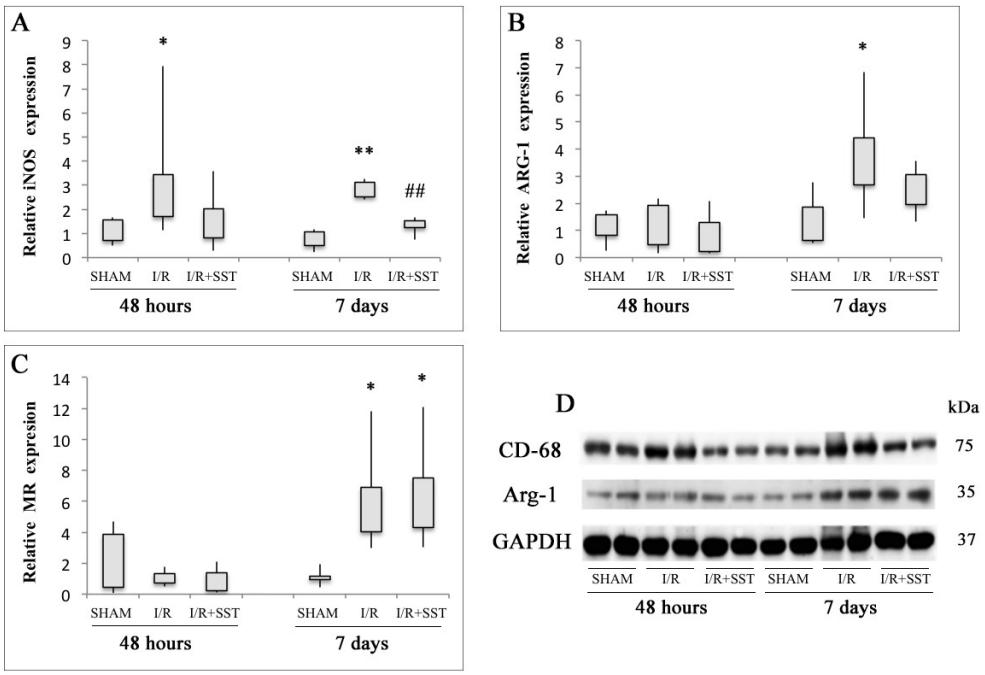

Fig. 20: Macrophage polarization *in vivo*, gene expression. Box plot representing relative expression levels of iNOS (A), Arg1 (B), and MR (C) evaluated by real-time PCR in renal tissue. Results were normalized to GAPDH expression. Graph represents two separate experiments performed in triplicate. *p<0.05, **p<0.001 vs. sham-treated animals, $^{\#\#}$p<0.001 vs. I/R. D) CD68 and Arg1 protein levels was measured by Western blot analysis in randomly selected samples of total kidney lysates. GAPDH was used as loading control.

To further confirm the involvement of HPSE in M1 macrophages polarization, we analysed the expression of genes encoding for proinflammatory cytokines TNF-α, IL-1β and IL-6 in mice kidney.

At both time points all three cytokines were significantly overexpressed in untreated ischemic mice, whilst they remained at basal levels in tissue from mice treated with SST0001 (Fig. 21A-C). These data were validated by western blot analysis (Fig. 21D).

However, the expression of M2 associated cytokine IL-10 was increased only 7 days after I/R injury in both untreated and treated mice (Fig. 21E).

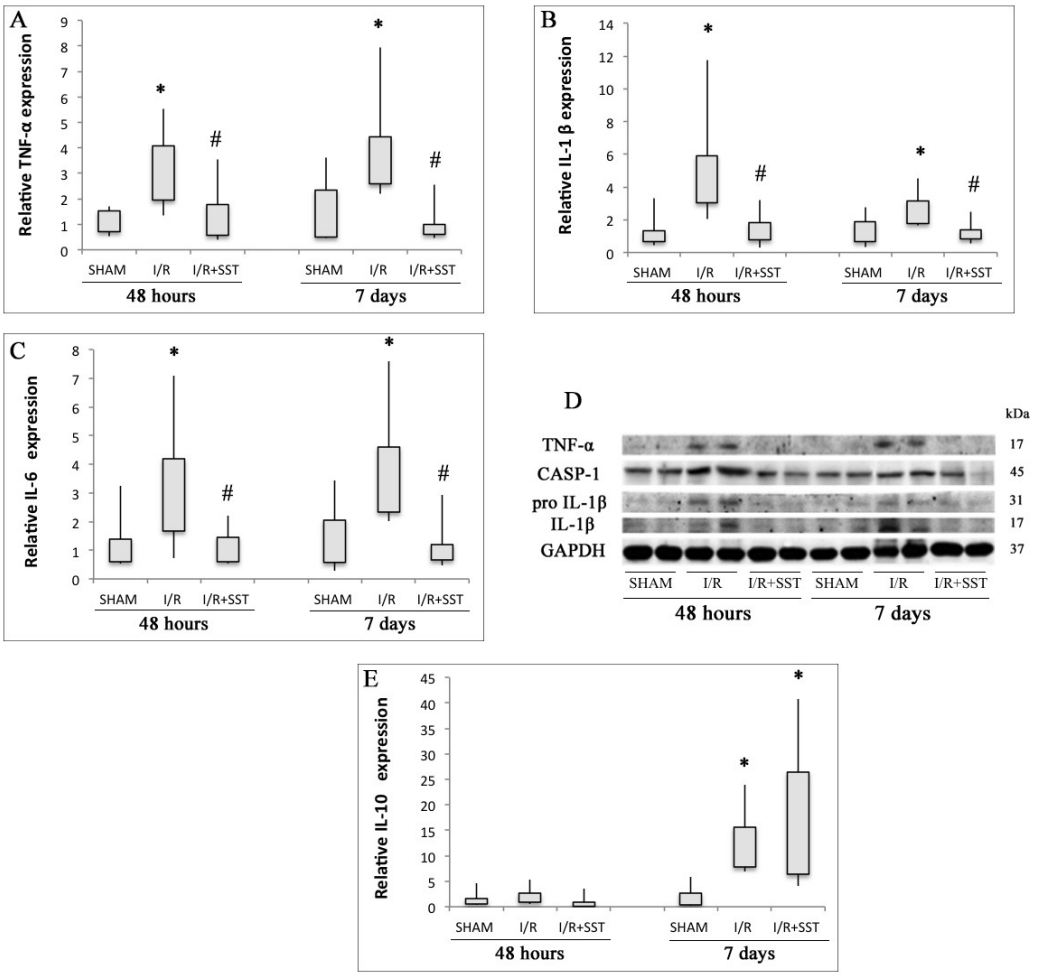

Fig. 21: Cytokine expression *in vivo*. Box plot representing relative expression levels of TNF-α (A), IL-1β (B), IL-6 (C), IL-10 (E), evaluated by real-time PCR in renal tissue. Results were normalized to GAPDH expression. Graph represents two separate experiments performed in triplicate. *P<0.05, **P<0.001 vs. sham-treated animals, $^{\#}$p<0.05, $^{\#\#}$p<0.001 vs. I/R. D) TNF-α, Caspase-1, and IL-1β protein levels measured by Western blot analysis in randomly selected samples of total kidney lysates. GAPDH was used as loading control.

I/R up-regulated the expression of TLR-2 and TLR-4 48 hours and 7 days after the ischemic damage only in mice not treated with the HPSE inhibitor, SST0001 treatment maintained their expression at basal levels (Fig. 22A-B).

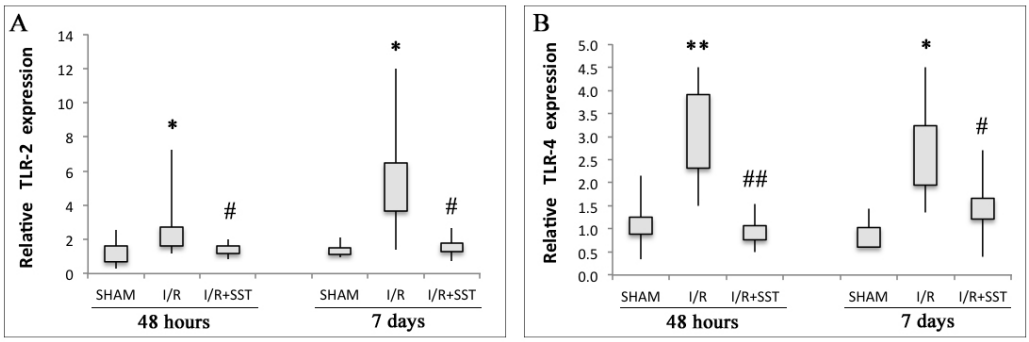

Fig. 22: TLRs expression *in vivo*. Box plot representing relative expression levels of TLR-2 (A) and TLR-4 (B) evaluated by real-time PCR in renal tissue. Results were normalized to GAPDH expression. Graph represents two separate experiments performed in triplicate. *$p<0.05$, *$p<0.001$ vs. sham-treated animals, $^{\#}p<0.05$, $^{\#\#}p<0.001$ vs. I/R.

4.2.3. HPSE inhibition decreased the number of apoptotic cells in renal parenchyma after I/R injury

To evaluate if the beneficial effects of HPSE inhibition was mediated also by preventing apoptosis, we measured the amount of apoptotic cells in kidney sections by TUNEL assay.

In the group of untreated mice, I/R caused a higher number of apoptotic cells compared to SST0001 treated mice (Fig. 23).

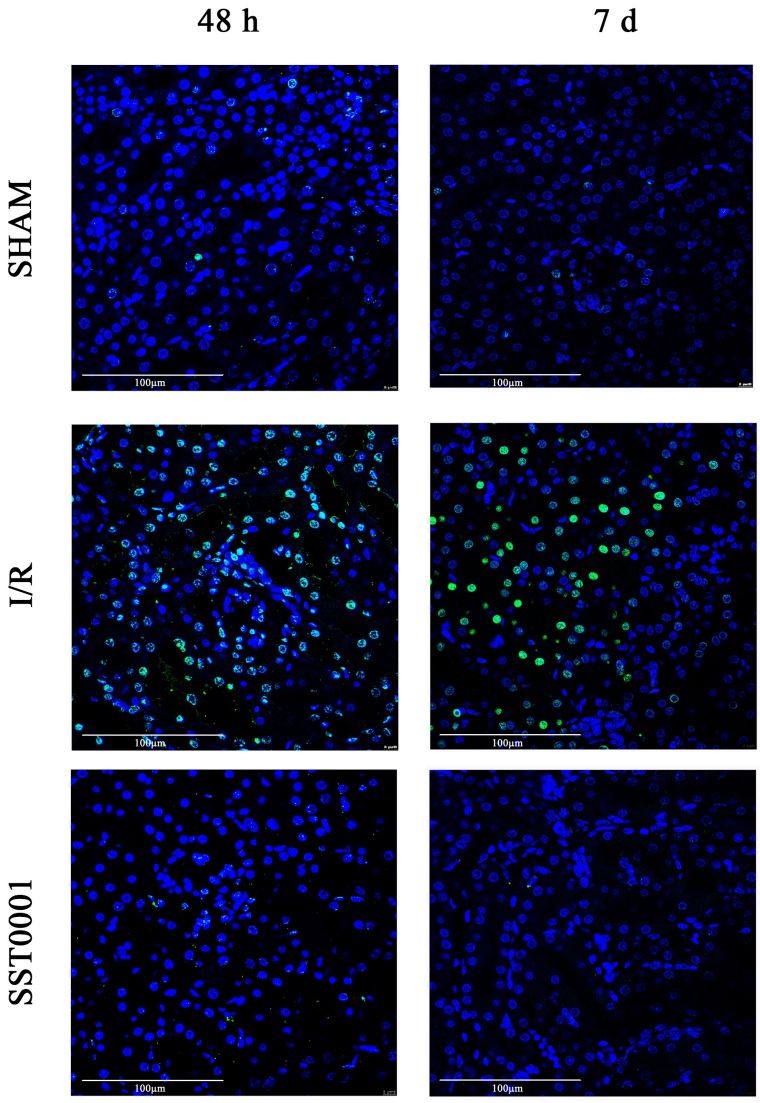

Fig. 23: Renal cell apoptosis after I/R injury. Renal cell apoptosis after renal I/R was evaluated by TUNEL staining. Apoptotic renal cells in post-I/R kidneys are green, and nuclei are shown in blue.

4.2.4. I/R injury affects kidney function that is preserved by HPSE inhibitor

I/R had a strong impact on renal function leading to a significantly increment of BUN and creatinine in serum of untreated mice 2 days after I/R injury, whereas the inhibition of HPSE seemed to preserve renal function in the early phase of the damage (Fig. 24A-B).

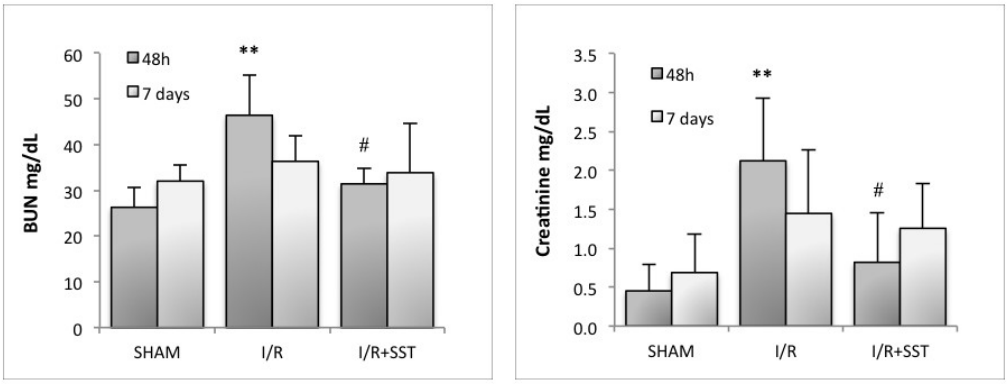

Fig. 24: Renal function in SST0001-treated and untreated mice subjected to I/R. Effects of I/R on (A) BUN and (B) serum creatinine after I/R measured in plasma from SST0001-treated and untreated mice. Results are expressed as mean ± SD: **p<0.001 vs. SHAM 48h; #p<0.001 vs. I/R 48 h I/R kidney injury.

Kidney sections were stained with Periodic Shiff-acid to visualize the kidney damage. Ischemic non-treated kidney presented tubular injury, as shown by the loss of brush border, tubules detachment from the basal membrane and the bubbling of tubular cells. These events were substantially reduced in kidney of mice treated with SST0001 (Fig. 25).

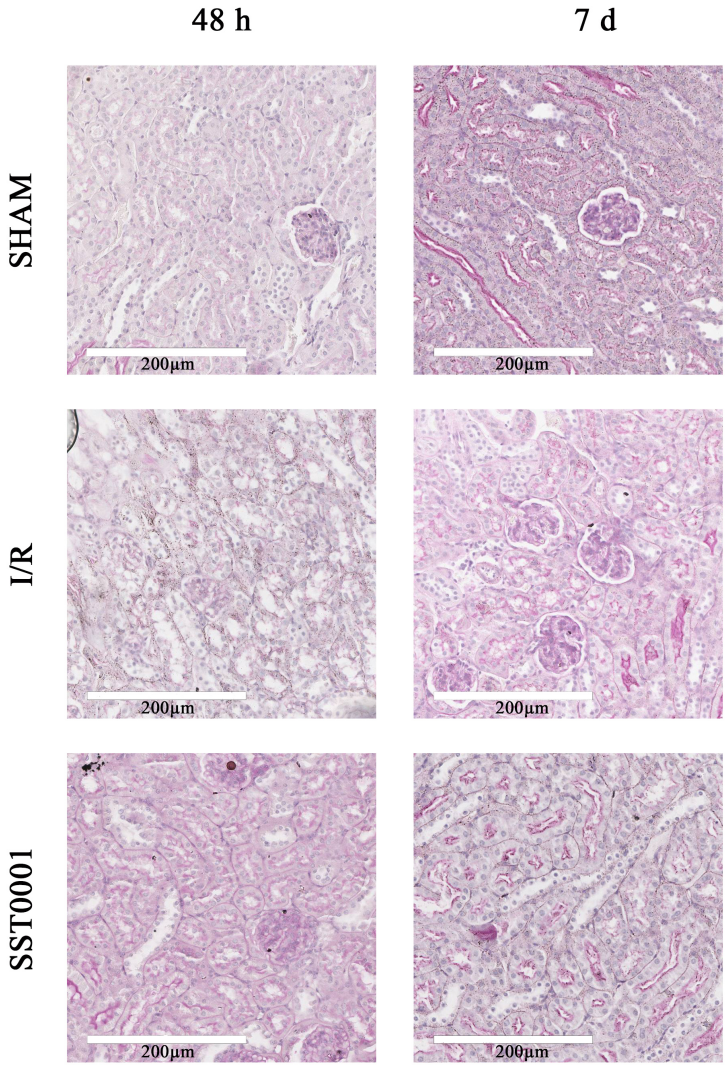

	Loss Brush Border	Sloughing	Blubbing
Sham 48h	0±0.0	0±0.0	0±0.0
I/R 48h	0.75±0.05	0.40±0.06	1.00±0.06
I/R + SST 48h	0.40±0.11	0.16±0.01	0.50±0.06
Sham 7 days	0±0.0	0±0.0	0±0.0
I/R 7 days	0±0.0	1.00±0.25	0.50±0.09
I/R + SST 7 days	0±0.0	0.20±0.06	0.66±0.07

Fig. 25: Histological PAS staining and score of renal tubular cell damage. Panels show representative images of PAS and H&E staining of paraffin-embedded cortex. Magnification 40X. Histopathological score was evaluated by a skilled pathologist in a blinded manner. Injury scale: 0 = <1% none, 1 = 1–25% mild, 2 = 25–50% moderate, 3 = 50–100% severe. Values are expressed as mean ± standard errors (SEM).

5. DISCUSSION

Renal transplantation is the gold standard therapy for patients with chronic renal failure but, unfortunately, some patients experience a delayed graft function (DGF), a clinical complication induced by I/R injury, that required early post-transplant dialysis treatment.

Many studies have shown that macrophages are involved in the troubled cellular network triggered by I/R by infiltrating into renal parenchyma and causing tissue damage. However, although well described, the biological mechanisms underlining this process are still only partially understood. We hypothesized that HPSE could have a role in the I/R injury-associated biological machinery in kidney. This enzyme is an endoglucuronidase that, cleaving HS chains, remodels the ECM and promotes the release of HS-bound cytokines and growth factors. By means of these activities HPSE has a role in renal EMT after I/R [95] as well as in other renal diseases [60, 65, 92, 98, 109-112]. It has been demonstrated that HPSE controls inflammation by regulating the recruitment of leucocytes and the interaction of these cells with endothelium, by modulating the bioavailability of cytokines in the extracellular matrix and by activating TLRs [90, 92, 113]. Therefore, it is plausible that this enzyme modulates also macrophages recruitment and their activation/polarization in kidney I/R.

In our study we investigated the relationship between HPSE and macrophages, and its role as a mediator in the crosstalk between macrophages and epithelial tubular cells in I/R kidney injury.

To this purpose, we started treating U937 cells with HPSE or SST0001 (the specific HPSE inhibitor) in the presence or absence of LPS and IL-4, two well-known M1 and M2 polarizing agents. Our results showed that HPSE has a role in macrophages activation/polarization, indeed it sustains M1 proinflammatory polarization and the production of proinflammatory cytokines (IL-1β, IL-6, TNF-α), whereas it does not influence M2 pro-regenerative polarization.

It is known that I/R can induce the activation of the innate immune response and cell death pathways in renal epithelial tubular cells leading to renal damage [114]. Cell death induces the release of DAMPs such as HMGB1 [115] that, in turn,

activate multiple receptors, including TLRs [114, 116] on macrophages and parenchymal cells sustaining inflammation [117-119]. As largely described in literature, during renal I/R injury, upregulation of TLR-2 and TLR-4 in renal tubular epithelial cells, vascular endothelial cells, and immunoinflammatory cells [120-122] facilitates the additional leukocyte migration and infiltration, activates the innate and adaptive immune responses and promotes the release of proinflammatory mediators, which in turn activate macrophages [123]. In this crosstalk between macrophages and renal epithelial tubular cells HPSE plays a key role. We demonstrated that in HK-2 cells exposed to H/R the upregulation of HPSE mediates the upregulation of TLR-2 and -4, the increment of apoptotic cells and the release of DAMPs such as HMGB1. HPSE increases the expression of TLRs also in macrophages, making them potentially more sensitive to the corresponding ligands. All these effects are minimized in the presence of SST0001. It is noteworthy that, although fragments of heparan sulfate can function as TLR ligands [124], the heparan sulfate mimetic SST0001 does not activate TLR signaling.

HPSE from HK-2 injured cells seems to facilitate the polarization of macrophages towards M1 phenotype. In fact, we found that conditioned medium from wild-type HK-2 cells after H/R can induce the expression of M1 markers in activated U937 cells, but the medium from HPSE-silenced cells does not have any effect. Nevertheless, these results should be confirmed in primary macrophages.

Furthermore, as previously reported I/R injury may induce a partial EMT in renal epithelial tubular cells. Our study revealed that the cytokines produced by M1 but not M2 macrophages mediate the EMT (Fig. 26). Contrarily, the lack of HPSE prevents it.

Future studies will be necessary to elucidate the biological bases of this process. In particular, it could be interesting to evaluate the effects of IL-1β, the principal cytokine produced by M1 macrophages, on partial EMT in tubular cells at the molecular level.

To validate *in vitro* results, we performed unilateral renal I/R injury by vascular clamping in mice in the presence or absence of SST0001 and we sacrificed them 2 or 7 days after I/R injury. As expected the *in vivo* part of the study showed

macrophages recruitment into the renal parenchyma during the early post-I/R phase (2 days), and confirmed the polarization towards M1 phenotype with an increased production of M1-associated pro-inflammatory cytokines. These cytokines sustain inflammation (e.g., IL-6) [121], cause parenchymal damage by inducing tubular cell death (e.g., TNF-a) [125], and activate fibrotic processes (e.g., IL-1β) [126, 127]. We also observed the upregulation of TLRs, which sustain the proinflammatory circuit [120-122]. Moreover, our *in vivo* experiments established that the inhibition of HPSE significantly decreases the infiltration of M1 macrophages, in turn reducing the production of proinflammatory and profibrotic cytokines, maintaining basal TLRs expression levels, and preventing I/R-induced tubular cell apoptosis, similarly to the *in vitro* results.

Seven days after I/R, we observed evidence of initial M2 polarization reflecting the initiation of a macrophage-dependent repair process. In fact, M2 macrophages produce anti-inflammatory and proregenerative mediators that modify the expression of several genes in parenchymal cells to promote tissue regeneration and repair [128, 129]. Our results support the evidence observed by an earlier *in vivo* study which show that the M2 polarization is regulated by specific cytokines (IL-4 and IL-10) produced during allograft processes characterized by the accumulation T helper 2 and regulatory T lymphocytes, probably enhanced by the infiltration of these cells along with M1 macrophages after the phagocytosis of apoptotic cells, and the production of cytokines such as colony-stimulating factor 1 by tubular cells [130].

The inhibition of HPSE by SST0001 does not reduce the M2 macrophage population or the expression of the M2 markers.

The specific reduction of the M1 component but not the M2 component by SST0001 is of great interest because it could provide a new strategy to control the initial inflammation that causes tissue damage without inhibiting M2 macrophages that facilitate repair. This was confirmed by our findings that SST0001 also ameliorates renal functions (BUN, creatinine, and histology) in mice subjected to I/R, and could in time achieve better organ recovery and the prevention of fibrosis.

A major limitation of our *in vivo* study is lack of a deep analysis of the biologic

elements implicated in the crosstalk between immune cells and renal (tubular and glomerular) compartment in an HPSE-dependent manner and vice versa.

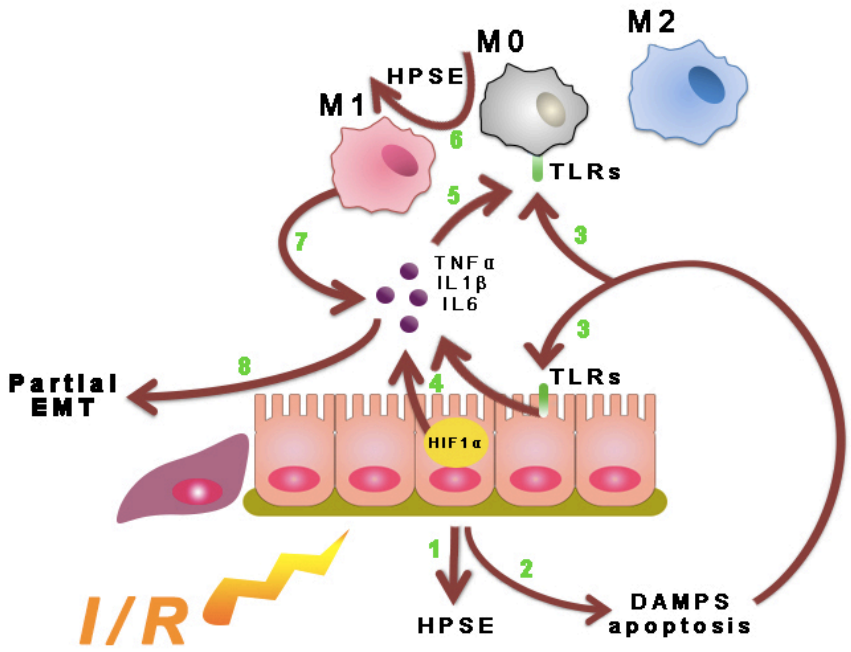

Fig. 26: Role of HPSE in macrophage polarization and crosstalk with tubular cells during I/R. Confirmed event induced by I/R injury is upregulation of HPSE at both tubular and glomerular levels (1). HPSE then induces tubular cell apoptosis and DAMP generation (2). DAMPs and molecules generated from necrotic cells can activate TLRs both on macrophages and tubular cells. HPSE also regulates TLR expression in both cell types (3). Tubular cells in response to direct hypoxic stimuli and TLR activation (4) produce proinflammatory cytokines (5) which attract and activate macrophages. This event is prevented by lack or inhibition of HPSE. High levels of HPSE facilitate M1 polarization of infiltrated macrophages (6). Additional re- lease of cytokines and growth factors (7) by macrophages (8) worsen parenchymal damage and sustain partial EMT of tubular cells, a condition that over time leads to fibrosis.

7. CONCLUSION

In conclusion, our study demonstrated that HPSE was a pivotal element involved in the complex renal biological machinery activated by I/R injury by regulating macrophages polarization/activation and the crosstalk between these immune-inflammatory cells and the renal tubular epithelium. Furthermore, it underlined that the inhibition of this enzyme, mitigating functional and morphological damages following I/R injury, could represent a new pharmacological tool in organ transplant medicine. Additional studies and trials are necessary to confirm our results in clinical setting.

8. ARTICLES PUBLISHED DURING DOCTORATE COURSE

- **Sulodexide alone or in combination with low doses of everolimus inhibits the hypoxia-mediated epithelial to mesenchymal transition in human renal proximal tubular cells.**

Gianluigi Zaza, Valentina Masola, Simona Granata, Gloria Bellin, Alessandra Dalla Gassa, Maurizio Onisto, Giovanni Gambaro, Antonio Lupo.

J Nephrol. 2015 Aug;28(4):431-40. doi: 10.1007/s40620-015-0216-y.

- **Epithelial to mesenchymal transition in the liver field: the double face of Everolimus in vitro.**

Valentina Masola, Amedeo Carraro, Gianluigi Zaza, Gloria Bellin, Umberto Montin, Paola Violi, Antonio Lupo and Umberto Tedeschi.

BMC Gastroenterol. 2015 Sep 14;15:118. doi: 10.1186/s12876-015-0347-6.

- **Transcriptomics: A Step behind the Comprehension of the Polygenic Influence on Oxidative Stress, Immune Deregulation, and Mitochondrial Dysfunction in Chronic Kidney Disease.**

Simona Granata, Alessandra Dalla Gassa, Gloria Bellin, Antonio Lupo, and Gianluigi Zaza.

Biomed Res Int. 2016;2016:9290857. doi: 10.1155/2016/9290857.

- **Heparanase: A Potential New Factor Involved in the Renal Epithelial Mesenchymal Transition (EMT) Induced by Ischemia/ Reperfusion (I/R) Injury.**

Valentina Masola, Gianluigi Zaza, Giovanni Gambaro, Maurizio Onisto, Gloria Bellin, Gisella Vischini, Iyad Khamaysi, Ahmad Hassan, Shadi Hamoud, Omri Nativ, Samuel N. Heyman, Antonio Lupo, Israel Vlodavsky, Zaid Abassi.

PLoS One. 2016 Jul 28;11(7):e0160074. doi: 10.1371/journal.pone.0160074.

- **Everolimus-induced epithelial to mesenchymal transition (EMT) in bronchial/pulmonary cells: when the dosage does matter in transplantation.**
Paola Tomei, Valentina Masola, Simona Granata, Gloria Bellin, Pierluigi Carratu`, Miriam Ficial, Valentina Anna Ventura, Maurizio Onisto, Onofrio Resta, Giovanni Gambaro, Marco Chilosi, Antonio Lupo, Gianluigi Zaza.
J Nephrol. 2016 Dec;29(6):881-891.

- **Specific heparanase inhibition reverses glucose-induced mesothelial-to-mesenchymal transition.**
Valentina Masola, Simona Granata, Gloria Bellin, Giovanni Gambaro, Maurizio Onisto, Carlo Rugiu, Antonio Lupo and Gianluigi Zaza.
Nephrol Dial Transplant. 2017 Jul 1;32(7):1145-1154. doi: 10.1093/ndt/gfw403.

- **Involvement of heparanase in the pathogenesis of acute kidney injury: nephroprotective effect of PG545.**
Zaid Abassi, Shadi Hamoud, Ahmad Hassan, Iyad Khamaysi, Omri Nativ, Samuel N. Heyman, Rabia Shekh Muhammad, Neta Ilan, Preeti Singh, Edward Hammond, Gianluigi Zaza, Antonio Lupo, Maurizio Onisto, Gloria Bellin, Valentina Masola, Israel Vlodavsky and Giovanni Gambaro.
Oncotarget. 2017 May 23;8(21):34191-34204. doi: 10.18632/oncotarget.16573.

- **Heparanase regulates the M1 polarization of renal macrophages and their crosstalk with renal epithelial tubular cells after ischemia/reperfusion injury.**
Valentina Masola, Gianluigi Zaza, Gloria Bellin, Luigi Dall'Olmo, Simona Granata, Gisella Vischini, Maria Francesca Secchi, Antonio Lupo, Giovanni Gambaro, and Maurizio Onisto.
FASEB J. 2017 Sep 28. pii: fj.201700597R. doi: 10.1096/fj.201700597R.

9. BIBLIOGRAPHY

1. Menke, J. et al. (2014) The effect of ischemia/reperfusion on the kidney graft. Curr Opin Organ Transplant 19 (4), 395-400.

2. Hotchkiss, R.S. et al. (2009) Cell death. N Engl J Med 361 (16), 1570-83.

3. Yellon, D.M. and Hausenloy, D.J. (2007) Myocardial reperfusion injury. N Engl J Med 357 (11), 1121-35.

4. Kalogeris, T. et al. (2012) Cell biology of ischemia/reperfusion injury. Int Rev Cell Mol Biol 298, 229-317.

5. Baines, C.P. (2009) The mitochondrial permeability transition pore and ischemia-reperfusion injury. Basic Res Cardiol 104 (2), 181-8.

6. Baines, C.P. (2009) The molecular composition of the mitochondrial permeability transition pore. J Mol Cell Cardiol 46 (6), 850-7.

7. Murphy, E. and Steenbergen, C. (2008) Ion transport and energetics during cell death and protection. Physiology (Bethesda) 23, 115-23.

8. Granger, D.N. and Kvietys, P.R. (2015) Reperfusion injury and reactive oxygen species: The evolution of a concept. Redox Biol 6, 524-51.

9. Kalogeris, T. et al. (2014) Mitochondrial reactive oxygen species: a double edged sword in ischemia/reperfusion vs preconditioning. Redox Biol 2, 702-14.

10. Hunot, S. and Flavell, R.A. (2001) Apoptosis. Death of a monopoly? Science 292 (5518), 865-6.

11. Borutaite, V. et al. (2003) Inhibition of mitochondrial permeability transition prevents mitochondrial dysfunction, cytochrome c release and apoptosis induced by heart ischemia. J Mol Cell Cardiol 35 (4), 357-66.

12. Yu, S.W. et al. (2002) Mediation of poly(ADP-ribose) polymerase-1-dependent cell death by apoptosis-inducing factor. Science 297 (5579), 259-63.

13. Daugas, E. et al. (2000) Mitochondrio-nuclear translocation of AIF in apoptosis and necrosis. Faseb j 14 (5), 729-39.

14. Eefting, F. et al. (2004) Role of apoptosis in reperfusion injury. Cardiovasc Res 61 (3), 414-26.

15. Przyklenk, K. et al. (2012) Autophagy as a therapeutic target for ischaemia /reperfusion injury? Concepts, controversies, and challenges. Cardiovasc Res 94 (2), 197-205.

16. Nathan, C. (2006) Neutrophils and immunity: challenges and opportunities. Nat Rev Immunol 6 (3), 173-82.

17. Phillipson, M. and Kubes, P. (2011) The neutrophil in vascular inflammation. Nat Med 17 (11), 1381-90.
18. Slegtenhorst, B.R. et al. (2014) Ischemia/reperfusion Injury and its Consequences on Immunity and Inflammation. Curr Transplant Rep 1 (3), 147-154.
19. Morelli, A.E. and Thomson, A.W. (2007) Tolerogenic dendritic cells and the quest for transplant tolerance. Nat Rev Immunol 7 (8), 610-21.
20. Tsung, A. et al. (2007) Increasing numbers of hepatic dendritic cells promote HMGB1-mediated ischemia-reperfusion injury. J Leukoc Biol 81 (1), 119-28.
21. Lanier, L.L. (2005) NK cell recognition. Annu Rev Immunol 23, 225-74.
22. Kim, H.J. et al. (2013) TLR2 signaling in tubular epithelial cells regulates NK cell recruitment in kidney ischemia-reperfusion injury. J Immunol 191 (5), 2657-64.
23. Kim, H.J. et al. (2012) Reverse signaling through the costimulatory ligand CD137L in epithelial cells is essential for natural killer cell-mediated acute tissue inflammation. Proc Natl Acad Sci U S A 109 (1), E13-22.
24. Cooper, D. et al. (2003) Time-dependent platelet-vessel wall interactions induced by intestinal ischemia-reperfusion. Am J Physiol Gastrointest Liver Physiol 284 (6), G1027-33.
25. Lam, F.W. et al. (2011) Platelets enhance neutrophil transendothelial migration via P-selectin glycoprotein ligand-1. Am J Physiol Heart Circ Physiol 300 (2), H468-75.
26. Geissmann, F. et al. (2010) Development of monocytes, macrophages, and dendritic cells. Science 327 (5966), 656-61.
27. Huen, S.C. and Cantley, L.G. (2017) Macrophages in Renal Injury and Repair. Annu Rev Physiol 79, 449-469.
28. Gordon, S. and Martinez, F.O. (2010) Alternative activation of macrophages: mechanism and functions. Immunity 32 (5), 593-604.
29. Cao, Q. et al. (2015) Macrophages in kidney injury, inflammation, and fibrosis. Physiology (Bethesda) 30 (3), 183-94.
30. Davis, M.J. et al. (2013) Macrophage M1/M2 polarization dynamically adapts to changes in cytokine microenvironments in Cryptococcus neoformans infection. MBio 4 (3), e00264-13.
31. Lee, S. et al. (2011) Distinct macrophage phenotypes contribute to kidney injury and repair. J Am Soc Nephrol 22 (2), 317-26.
32. Perico, N. et al. (2004) Delayed graft function in kidney transplantation. Lancet 364 (9447), 1814-27.

33. Ojo, A.O. et al. (1997) Delayed graft function: risk factors and implications for renal allograft survival. Transplantation 63 (7), 968-74.
34. Shoskes, D.A. and Cecka, J.M. (1998) Deleterious effects of delayed graft function in cadaveric renal transplant recipients independent of acute rejection. Transplantation 66 (12), 1697-701.
35. Troppmann, C. et al. (1995) Delayed graft function, acute rejection, and outcome after cadaver renal transplantation. The multivariate analysis. Transplantation 59 (7), 962-8.
36. Yarlagadda, S.G. et al. (2009) Association between delayed graft function and allograft and patient survival: a systematic review and meta-analysis. Nephrol Dial Transplant 24 (3), 1039-47.
37. Koning, O.H. et al. (1997) Risk factors for delayed graft function in cadaveric kidney transplantation: a prospective study of renal function and graft survival after preservation with University of Wisconsin solution in multi-organ donors. European Multicenter Study Group. Transplantation 63 (11), 1620-8.
38. Ojo, A.O. et al. (2000) Long-term survival in renal transplant recipients with graft function. Kidney Int 57 (1), 307-13.
39. Irish, W.D. et al. (2010) A risk prediction model for delayed graft function in the current era of deceased donor renal transplantation. Am J Transplant 10 (10), 2279-86.
40. Jeldres, C. et al. (2009) Prediction of delayed graft function after renal transplantation. Can Urol Assoc J 3 (5), 377-82.
41. Rodrigo, E. et al. (2012) Prediction of delayed graft function by means of a novel web-based calculator: a single-center experience. Am J Transplant 12 (1), 240-4.
42. Loverre, A. et al. (2011) T helper 1, 2 and 17 cell subsets in renal transplant patients with delayed graft function. Transpl Int 24 (3), 233-42.
43. Zaza, G. et al. (2014) Karyopherins: potential biological elements involved in the delayed graft function in renal transplant recipients. BMC Med Genomics 7, 14.
44. Beg, A.A. (2002) Endogenous ligands of Toll-like receptors: implications for regulating inflammatory and immune responses. Trends Immunol 23 (11), 509-12.
45. Aliprantis, A.O. et al. (2000) The apoptotic signaling pathway activated by Toll-like receptor-2. Embo j 19 (13), 3325-36.
46. Danobeitia, J.S. et al. (2014) The role of complement in the pathogenesis of renal ischemia-reperfusion injury and fibrosis. Fibrogenesis Tissue Repair 7, 16.
47. Nieto, M.A. et al. (2016) EMT: 2016. Cell 166 (1), 21-45.

48. Lv, Q. et al. (2016) The advancements of heparanase in fibrosis. Int J Mol Epidemiol Genet 7 (4), 137-140.
49. Secchi, M.F. et al. (2015) Recent data concerning heparanase: focus on fibrosis, inflammation and cancer. Biomol Concepts 6 (5-6), 415-21.
50. He, W. and Dai, C. (2015) Key Fibrogenic Signaling. Curr Pathobiol Rep 3 (2), 183-192.
51. Liu, Y. (2010) New insights into epithelial-mesenchymal transition in kidney fibrosis. J Am Soc Nephrol 21 (2), 212-22.
52. Jang, H.R. and Rabb, H. (2009) The innate immune response in ischemic acute kidney injury. Clin Immunol 130 (1), 41-50.
53. Awad, A.S. et al. (2009) Compartmentalization of neutrophils in the kidney and lung following acute ischemic kidney injury. Kidney Int 75 (7), 689-98.
54. Oh, D.J. et al. (2008) Fractalkine receptor (CX3CR1) inhibition is protective against ischemic acute renal failure in mice. Am J Physiol Renal Physiol 294 (1), F264-71.
55. Anders, H.J. and Ryu, M. (2011) Renal microenvironments and macrophage phenotypes determine progression or resolution of renal inflammation and fibrosis. Kidney Int 80 (9), 915-25.
56. Ko, G.J. et al. (2008) Macrophages contribute to the development of renal fibrosis following ischaemia/reperfusion-induced acute kidney injury. Nephrol Dial Transplant 23 (3), 842-52.
57. Meng, X.M. et al. (2015) Macrophage Phenotype in Kidney Injury and Repair. Kidney Dis (Basel) 1 (2), 138-46.
58. Vlodavsky, I. and Friedmann, Y. (2001) Molecular properties and involvement of heparanase in cancer metastasis and angiogenesis. J Clin Invest 108 (3), 341-7.
59. Hulett, M.D. et al. (2000) Identification of active-site residues of the pro-metastatic endoglycosidase heparanase. Biochemistry 39 (51), 15659-67.
60. Rivara, S. et al. (2016) Heparanase: a rainbow pharmacological target associated to multiple pathologies including rare diseases. Future Med Chem 8 (6), 647-80.
61. Vlodavsky, I. et al. (2007) Heparanase: structure, biological functions, and inhibition by heparin-derived mimetics of heparan sulfate. Curr Pharm Des 13 (20), 2057-73.
62. Gong, F. et al. (2003) Processing of macromolecular heparin by heparanase. J Biol Chem 278 (37), 35152-8.
63. Dong, J. et al. (2000) Genomic organization and chromosome localization of the newly identified human heparanase gene. Gene 253 (2), 171-8.

64. Baraz, L. et al. (2006) Tumor suppressor p53 regulates heparanase gene expression. Oncogene 25 (28), 3939-47.
65. Rabelink, T.J. et al. (2017) Heparanase: roles in cell survival, extracellular matrix remodelling and the development of kidney disease. Nat Rev Nephrol 13 (4), 201-212.
66. Shteingauz, A. et al. (2014) Processing of heparanase is mediated by syndecan-1 cytoplasmic domain and involves syntenin and alpha-actinin. Cell Mol Life Sci 71 (22), 4457-70.
67. Cohen, E. et al. (2005) Heparanase processing by lysosomal/endosomal protein preparation. FEBS Lett 579 (11), 2334-8.
68. Fairbanks, M.B. et al. (1999) Processing of the human heparanase precursor and evidence that the active enzyme is a heterodimer. J Biol Chem 274 (42), 29587-90.
69. Wu, L. et al. (2015) Structural characterization of human heparanase reveals insights into substrate recognition. Nat Struct Mol Biol 22 (12), 1016-22.
70. Nardella, C. et al. (2004) Mechanism of activation of human heparanase investigated by protein engineering. Biochemistry 43 (7), 1862-73.
71. Fux, L. et al. (2009) Structure-function approach identifies a COOH-terminal domain that mediates heparanase signaling. Cancer Res 69 (5), 1758-67.
72. Levy-Adam, F. et al. (2005) Identification and characterization of heparin/heparan sulfate binding domains of the endoglycosidase heparanase. J Biol Chem 280 (21), 20457-66.
73. Vlodavsky, I. et al. (2016) Heparanase: From basic research to therapeutic applications in cancer and inflammation. Drug Resist Updat 29, 54-75.
74. Gandhi, N.S. et al. (2012) Computational analyses of the catalytic and heparin-binding sites and their interactions with glycosaminoglycans in glycoside hydrolase family 79 endo-beta-D-glucuronidase (heparanase). Glycobiology 22 (1), 35-55.
75. Peterson, S.B. and Liu, J. (2013) Multi-faceted substrate specificity of heparanase. Matrix Biol 32 (5), 223-7.
76. Weissmann, M. et al. (2016) Heparanase-neutralizing antibodies attenuate lymphoma tumor growth and metastasis. Proc Natl Acad Sci U S A 113 (3), 704-9.
77. Edovitsky, E. et al. (2004) Heparanase gene silencing, tumor invasiveness, angiogenesis, and metastasis. J Natl Cancer Inst 96 (16), 1219-30.
78. Huining, L. et al. (2013) Inhibition of choriocarcinoma by Fe3O4-dextran-anti-beta-human chorionic gonadotropin nanoparticles containing antisense oligodeoxynucleotide of heparanase. Int J Nanomedicine 8, 4371-8.

79. Simmons, S.C. et al. (2012) Development of novel single-stranded nucleic acid aptamers against the pro-angiogenic and metastatic enzyme heparanase (HPSE1). PLoS One 7 (6), e37938.
80. Fu, J. et al. (2012) Heparanase DNA vaccine delivered by electroporation induces humoral immunity and cytoimmunity in animal models. Vaccine 30 (12), 2187-96.
81. Naggi, A. et al. (2005) Modulation of the heparanase-inhibiting activity of heparin through selective desulfation, graded N-acetylation, and glycol splitting. J Biol Chem 280 (13), 12103-13.
82. Ferro, V. et al. (2012) Discovery of PG545: a highly potent and simultaneous inhibitor of angiogenesis, tumor growth, and metastasis. J Med Chem 55 (8), 3804-13.
83. Winterhoff, B. et al. (2015) PG545 enhances anti-cancer activity of chemotherapy in ovarian models and increases surrogate biomarkers such as VEGF in preclinical and clinical plasma samples. Eur J Cancer 51 (7), 879-892.
84. Nasser, N.J. (2008) Heparanase involvement in physiology and disease. Cell Mol Life Sci 65 (11), 1706-15.
85. Goldberg, R. et al. (2013) Versatile role of heparanase in inflammation. Matrix Biol 32 (5), 234-240.
86. Axelsson, J. et al. (2012) Inactivation of heparan sulfate 2-O-sulfotransferase accentuates neutrophil infiltration during acute inflammation in mice. Blood 120 (8), 1742-51.
87. Bode, J.G. et al. (2012) The macrophage response towards LPS and its control through the p38(MAPK)-STAT3 axis. Cell Signal 24 (6), 1185-94.
88. Gotte, M. (2003) Syndecans in inflammation. Faseb j 17 (6), 575-91.
89. Parish, C.R. (2006) The role of heparan sulphate in inflammation. Nat Rev Immunol 6 (9), 633-43.
90. Blich, M. et al. (2013) Macrophage activation by heparanase is mediated by TLR-2 and TLR-4 and associates with plaque progression. Arterioscler Thromb Vasc Biol 33 (2), e56-65.
91. Lerner, I. et al. (2011) Heparanase powers a chronic inflammatory circuit that promotes colitis-associated tumorigenesis in mice. J Clin Invest 121 (5), 1709-21.
92. Goldberg, R. et al. (2014) Role of heparanase-driven inflammatory cascade in pathogenesis of diabetic nephropathy. Diabetes 63 (12), 4302-13.
93. Lider, O. et al. (1989) Suppression of experimental autoimmune diseases and prolongation of allograft survival by treatment of animals with low doses of heparins. J Clin Invest 83 (3), 752-6.

94. Vlodavsky, I. et al. (1992) Expression of heparanase by platelets and circulating cells of the immune system: possible involvement in diapedesis and extravasation. Invasion Metastasis 12 (2), 112-27.
95. Masola, V. et al. (2016) Heparanase: A Potential New Factor Involved in the Renal Epithelial Mesenchymal Transition (EMT) Induced by Ischemia/Reperfusion (I/R) Injury. PLoS One 11 (7), e0160074.
96. Loeffler, I. and Wolf, G. (2014) Transforming growth factor-beta and the progression of renal disease. Nephrol Dial Transplant 29 Suppl 1, i37-i45.
97. Masola, V. et al. (2012) Heparanase and syndecan-1 interplay orchestrates fibroblast growth factor-2-induced epithelial-mesenchymal transition in renal tubular cells. J Biol Chem 287 (2), 1478-88.
98. Masola, V. et al. (2011) Regulation of heparanase by albumin and advanced glycation end products in proximal tubular cells. Biochim Biophys Acta 1813 (8), 1475-82.
99. Gil, N. et al. (2012) Heparanase is essential for the development of diabetic nephropathy in mice. Diabetes 61 (1), 208-16.
100. Abassi, Z. et al. (2017) Involvement of heparanase in the pathogenesis of acute kidney injury: nephroprotective effect of PG545. Oncotarget 8 (21), 34191-34204.
101. Celie, J.W. et al. (2007) Subendothelial heparan sulfate proteoglycans become major L-selectin and monocyte chemoattractant protein-1 ligands upon renal ischemia/reperfusion. Am J Pathol 170 (6), 1865-78.
102. Song, M.G. et al. (2015) NRF2 Signaling Negatively Regulates Phorbol-12-Myristate-13-Acetate (PMA)-Induced Differentiation of Human Monocytic U937 Cells into Pro-Inflammatory Macrophages. PLoS One 10 (7), e0134235.
103. Gutter-Kapon, L. et al. (2016) Heparanase is required for activation and function of macrophages. Proc Natl Acad Sci U S A 113 (48), E7808-e7817.
104. Yu, M. et al. (2006) HMGB1 signals through toll-like receptor (TLR) 4 and TLR2. Shock 26 (2), 174-9.
105. Meirovitz, A. et al. (2013) Heparanase in inflammation and inflammation-associated cancer. Febs j 280 (10), 2307-19.
106. Goodall, K.J. et al. (2014) Soluble heparan sulfate fragments generated by heparanase trigger the release of pro-inflammatory cytokines through TLR-4. PLoS One 9 (10), e109596.
107. Zuk, A. and Bonventre, J.V. (2016) Acute Kidney Injury. Annu Rev Med 67, 293-307.

108. Zhang, M. et al. (2005) Interleukin-1beta-induced transdifferentiation of renal proximal tubular cells is mediated by activation of JNK and p38 MAPK. Nephron Exp Nephrol 99 (3), e68-76.
109. Garsen, M. et al. (2016) Heparanase Is Essential for the Development of Acute Experimental Glomerulonephritis. Am J Pathol 186 (4), 805-15.
110. Masola, V. et al. (2012) A new mechanism of action of sulodexide in diabetic nephropathy: inhibits heparanase-1 and prevents FGF-2-induced renal epithelial-mesenchymal transition. J Transl Med 10, 213.
111. Masola, V. et al. (2015) Impact of heparanase on renal fibrosis. J Transl Med 13, 181.
112. Zaza, G. et al. (2014) Dialysis-related transcriptomic profiling: the pivotal role of heparanase. Exp Biol Med (Maywood) 239 (1), 52-64.
113. Sedeek, M. et al. (2013) NADPH oxidases, reactive oxygen species, and the kidney: friend and foe. J Am Soc Nephrol 24 (10), 1512-8.
114. Zhang, J. et al. (2016) HMGB1-TLR4 signaling participates in renal ischemia reperfusion injury and could be attenuated by dexamethasone-mediated inhibition of the ERK/NF-kappaB pathway. Am J Transl Res 8 (10), 4054-4067.
115. Park, J.S. et al. (2003) Activation of gene expression in human neutrophils by high mobility group box 1 protein. Am J Physiol Cell Physiol 284 (4), C870-9.
116. Andersson, U. et al. (2000) High mobility group 1 protein (HMG-1) stimulates proinflammatory cytokine synthesis in human monocytes. J Exp Med 192 (4), 565-70.
117. Liu, X.J. et al. (2014) Proximal tubule toll-like receptor 4 expression linked to inflammation and apoptosis following hypoxia/reoxygenation injury. Am J Nephrol 39 (4), 337-47.
118. Pedregosa, J.F. et al. (2011) TLR2 and TLR4 expression after kidney ischemia and reperfusion injury in mice treated with FTY720. Int Immunopharmacol 11 (9), 1311-8.
119. Zhao, H. et al. (2014) Role of Toll-like receptor-4 in renal graft ischemia-reperfusion injury. Am J Physiol Renal Physiol 306 (8), F801-11.
120. Sanchez-Nino, M.D. et al. (2010) TNF superfamily: a growing saga of kidney injury modulators. Mediators Inflamm 2010.
121. Vesey, D.A. et al. (2002) Interleukin-1beta stimulates human renal fibroblast proliferation and matrix protein production by means of a transforming growth factor-beta-dependent mechanism. J Lab Clin Med 140 (5), 342-50.

122. Vesey, D.A. et al. (2002) Interleukin-1beta induces human proximal tubule cell injury, alpha-smooth muscle actin expression and fibronectin production. Kidney Int 62 (1), 31-40.
123. Chen, G.Y. and Nunez, G. (2010) Sterile inflammation: sensing and reacting to damage. Nat Rev Immunol 10 (12), 826-37.
124. Rabadi, M.M. et al. (2012) HMGB1 in renal ischemic injury. Am J Physiol Renal Physiol 303 (6), F873-85.
125. Mantovani, A. et al. (2004) The chemokine system in diverse forms of macrophage activation and polarization. Trends Immunol 25 (12), 677-86.
126. Wang, Y. et al. (2015) Proximal tubule-derived colony stimulating factor-1 mediates polarization of renal macrophages and dendritic cells, and recovery in acute kidney injury. Kidney Int 88 (6), 1274-1282.
127. Wynn, T.A. (2004) Fibrotic disease and the T(H)1/T(H)2 paradigm. Nat Rev Immunol 4 (8), 583-94.
128. Zaza, G. et al. (2015) Sulodexide alone or in combination with low doses of everolimus inhibits the hypoxia-mediated epithelial to mesenchymal transition in human renal proximal tubular cells. J Nephrol 28 (4), 431-40.
129. Minafra, L. et al. (2011) Proteomic differentiation pattern in the U937 cell line. Leuk Res 35 (2), 226-36.
130. Taniguchi, K. et al. (2015) Essential Role of Lysophosphatidylcholine Acyltransferase 3 in the Induction of Macrophage Polarization in PMA-Treated U937 Cells. J Cell Biochem 116 (12), 2840-8.